The Journal of Antibiotics (2012) 65, 211–214

www.nature.com/ja

NOTE

Napyradiomycin A1, an inhibitor of mitochondrial complexes I and II

Kohta Yamamoto[1], Etsu Tashiro[1], Keiichiro Motohashi[2], Haruo Seto[2] and Masaya Imoto[1]

The Journal of Antibiotics (2012) **65**, 211–214; doi:10.1038/ja.2011.138; published online 18 January 2012

Keywords: mitochondrial electron transport; napyradiomycin; intracellular ATP level

We have previously proposed a cell-based screening method 'EGF-induced (epidermal growth factor) filopodium protrusion assay' to identify mitochondrial electron transport inhibitors or glycolysis inhibitors. Filopodia are spike-like cell membrane projections that contribute to tumor metastasis. Previously, we have reported that mitochondrial electron transport inhibition resulted in the inhibition of EGF-induced filopodium protrusion in human adenocarcinoma A431 cells only when their glycolytic pathways were restricted.[1] By using the inhibition of filopodium protrusion as an indicator, we identified napyradiomycin A1 (Figure 1a; isolated from *Streptomyces antimycoticus* NT17),[2] which was previously identified as an antibacterial antibiotic,[3] as a candidate of mitochondrial electron transport inhibitor. A431 cells were treated with napyradiomycin A1 with or without 10 mM 2-deoxy-D-glucose (Sigma-Aldrich, St Louis, MO, USA) for 30 min, followed by 30 ng ml^{-1} EGF (Sigma-Aldrich) stimulation and observation under a microscope. As shown in Figure 1b, 20 μM napyradiomycin A1 inhibited EGF-induced filopodium protrusion in A431 cells only in the presence of the glycolytic enzyme hexokinase inhibitor 2-deoxy-D-glucose. Mitochondrial electron transport inhibitor rotenone (Sigma-Aldrich) also inhibited filopodium protrusion only in the presence of 2-deoxy-D-glucose. Furthermore, it was reported that co-treatment with a mitochondrial electron transport inhibitor and a glycolytic inhibitor markedly decreased intracellular ATP levels.[1] We then tested whether napyradiomycin A1 decreased ATP levels in A431 cells in which glycolytic pathways were restricted. As intracellular ATP levels were not affected by EGF stimulation (data not shown), we measured intracellular ATP levels under the condition where A431 cells were treated with napyradiomycin A1 with or without 10 mM 2-deoxy-D-glucose for 30 min in the absence of EGF. After incubation, intracellular ATP levels were measured using a Cell Titer-Glo Luminescent Cell Viability Assay Kit (Promega, Madison, WI, USA) with a luminometer (Wallac; Perkin-Elmer, Waltham, MA, USA). As shown in Figure 1c, napyradiomycin A1 treatment did not decrease cellular ATP levels; however, 20 μM napyradiomycin A1 markedly decreased cellular ATP levels in the presence of 2-deoxy-D-glucose in A431 cells. Furthermore, ATP levels in HeLa cells also decreased under co-treatment with napyradiomycin A1 and 2-deoxy-D-glucose (data not shown). These results suggested that napyradiomycin A1 inhibited mitochondrial electron transport in cancer cells.

Next, we examined whether napyradiomycin A1 actually inhibited mitochondrial electron transport *in vitro* by using submitochondrial particles (SMP) obtained from the bovine heart. In order to prepare SMP, bovine hearts were homogenized in MSH buffer (210 mM mannitol, 70 mM sucrose, 1 mM DTT, 1 mM EGTA, 0.1% BSA and 10 mM HEPES pH 7.4) with a Potter-Elvehjem homogenizer (Nippon genetics, Tokyo, Japan). Homogenates were centrifuged at 1000 *g* for 10 min, and the resulting supernatant was further centrifuged at 8000 *g* for 20 min. Pellets were suspended in MSH buffer and obtained as SMP.[4]

The mitochondrial electron transport chain consists of four discrete multisubunit complexes: NADH–ubiquinone oxidoreductase (complex I), succinate–ubiquinone oxidoreductase (complex II), ubiquinol–cytochrome *c* oxidoreductase (complex III) and cytochrome *c* oxidase (complex IV). Therefore, we evaluated which complex was the target of napyradiomycin A1.

Mitochondrial complex I activity was measured by monitoring the absorbance change of NADH at 340 nm in the presence of antimycin A (Sigma-Aldrich) and KCN (Sigma-Aldrich), an inhibitor of complex III and complex IV, respectively.[5,6] The enzyme assay was performed at 30 °C in a buffer containing 50 mM phosphate (pH 7.4), 250 mM sucrose, 0.1 μg ml^{-1} antimycin A, 2 mM KCN, 50 μM decylubiquinone (DB; 2,3-dimethoxy-5-methyl-6-decyl-1,4-benzoquinone, an exogenous hydrophobic quinone that acts as electron acceptor; Sigma-Aldrich),[7] 0.2 mM NADH, and 12 μg ml^{-1} SMP with or without napyradiomycin A1. Rotenone was used as a positive control of complex I inhibitor. We found that napyradiomycin A1 inhibited complex I activity with an IC_{50} value of 20 μM (Figure 2a).

[1]Chemical Biology Laboratory, Department of Biosciences and Informatics, Faculty of Science and Technology, Keio University, Yokohama City, Japan and [2]Bioregulatory Laboratory, Faculty of Applied Biosciences, Tokyo University of Agriculture, Tokyo, Japan
Correspondence: Dr E Tashiro, Department of Biosciences and Informatics, Faculty of Science and Technology, Chemical Biology Laboratory, Faculty of Science and Technology, Keio University, 3-14-1 Hiyoshi, Kohoku-ku, Yokohama 223-8522, Japan.
E-mail: tashiro@bio.keio.ac.jp
Received 2 December 2011; revised 15 December 2011; accepted 16 December 2011; published online 18 January 2012

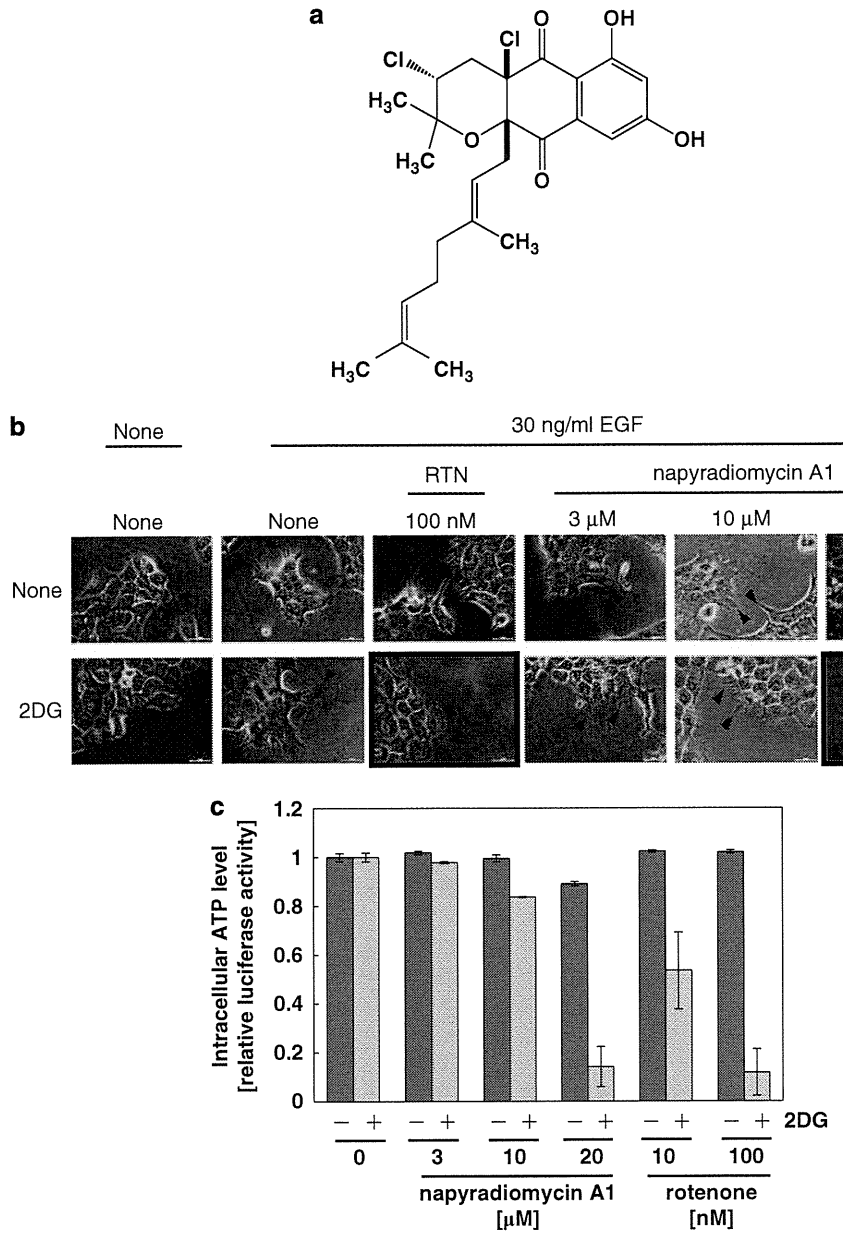

Figure 1 Napyradiomycin A1 decreased intracellular ATP levels. (**a**) The structure of napyradiomycin A1.[3] (**b**) Napyradiomycin A1 inhibited EGF-induced filopodia protrusion only in the presence of 2-deoxy-D-glucose (2DG, 10 mM). The assay method was as described previously.[1] Mitochondrial electron transport inhibitor rotenone (RTN 100 nM) was used as a positive control. Arrowhead indicates filopodia, and the framed photos show filopodium inhibition. (**c**) Napyradiomycin A1 decreased intracellular ATP levels in 2DG-treated A431 cells. A431 cells were treated with napyradiomycin A1 with or without 10 mM of 2DG for 30 min. After incubation, intracellular ATP levels were measured using a Cell Titer-Glo Luminescent Cell Viability Assay Kit with a luminometer.

Mitochondrial complex II activity was measured by monitoring the absorbance change of 2,6-dichlorophenolindophenol (Sigma-Aldrich) at 600 nm in the presence of rotenone and KCN.[8] The enzyme assay was performed at 30 °C in a buffer containing 50 mM phosphate (pH 7.4), 0.1 μM rotenone, 2 mM KCN, 40 μM 2,6-dichlorophenolindophenol, and 12 μg ml^{-1} SMP with or without napyradiomycin A1. Theonoyl trifluoroacetone (Sigma-Aldrich) was used as a positive control of complex II inhibitor.[9] We found that napyradiomycin A1 inhibited complex II activity with an IC_{50} value of 9.7 μM (Figure 2b).

Mitochondrial complex III activity was measured by monitoring the absorbance change of the reduction of oxidized cytochrome *c* at 550 nm in the presence of rotenone, KCN and an electron donor decylubiquinol. Decylubiquinol was obtained by the reduction of DB with sodium borohydride.[10] The enzyme assay was performed at 30 °C in a buffer containing 50 mM Tris (pH 7.6), 1 mM $MgCl_2$, 0.1 μM rotenone, 2 mM KCN, 40 μM cytochrome *c*, 50 μM decylubiquinol and 12 μg ml^{-1} SMP with or without napyradiomycin A1. Although antimycin A inhibited complex III activity, napyradiomycin A1 did not, even at 20 μM (Figure 2c)

Mitochondrial complex IV activity was measured by monitoring the absorbance change of the oxidation of reduced cytochrome *c* at 550 nm. The enzyme assay was performed at 30 °C in a buffer containing 50 mM Tris (pH 7.6), 1 mM $MgCl_2$, 0.1 μg ml^{-1} antimycin A, 0.1 μM rotenone, 20 μM reduced cytochrome *c* and 12 μg ml^{-1} SMP

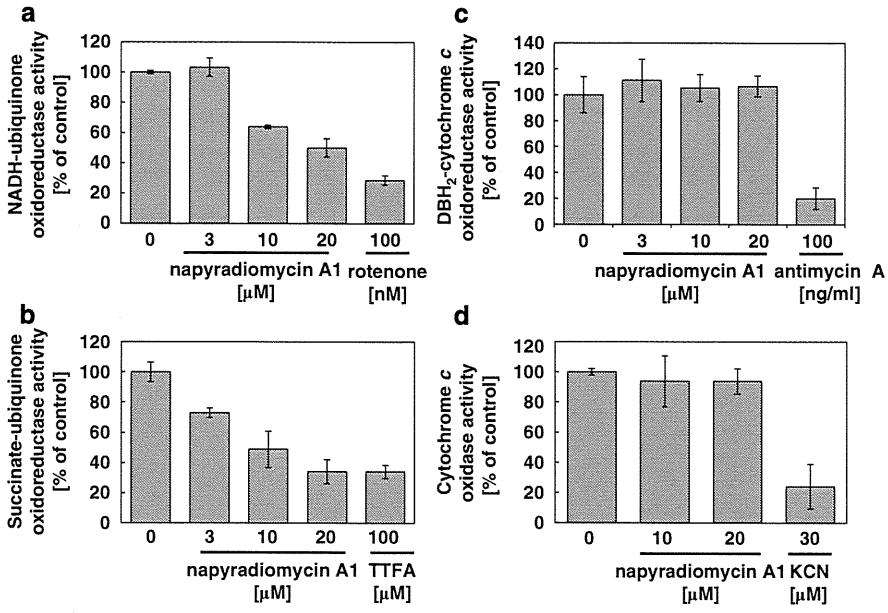

Figure 2 Napyradiomycin A1 inhibited mitochondrial complexes I and II. A modification of previously reported methods[10,16–18] was used to measure complex I, complex II, complex III and complex IV activities. (**a**) Napyradiomycin A1 inhibited complex I activity. Mitochondrial complex I (NADH–ubiquinone oxidoreductase) activity was measured by monitoring the absorbance change of NADH at 340 nm using SMP. (**b**) Napyradiomycin A1 inhibited complex II activity. Mitochondrial complex II (Succinate–ubiquinone oxidoreductase) activity was measured by monitoring the absorbance change of 2,6-dichlorophenolindophenol at 600 nm using SMP. (**c**) Napyradiomycin A1 did not inhibit complex III activity. Mitochondrial complex III (decylubiquinol (DBH_2)–cytochrome *c* oxidoreductase) activity was measured by monitoring the absorbance change of cytochrome *c* at 550 nm using SMP. (**d**) Napyradiomycin A1 did not inhibit complex IV activity. Mitochondrial complex IV (cytochrome *c* oxidase) activity was measured by monitoring the absorbance change of the oxidation of reduced cytochrome *c* at 550 nm using SMP. SMP were obtained by standard different centrifugation.[4] All data are the mean ± s.d. of three independent experiments.

with or without napyradiomycin A1. Although KCN inhibited complex IV activity, 20 μM napyradiomycin A1 inhibited complex IV activity less than 10% (Figure 2d).

In conclusion, napyradiomycin A1 inhibited mitochondrial complexes I and II, but did not inhibit complex III or IV *in vitro*. Therefore, it was suggested that mitochondrial electron transport inhibition by napyradiomycin A1 was caused by the inhibition of mitochondrial complexes I and II.

It was reported that the isoprenyl unit of ubiquinone was important to bind to mitochondrial complex I.[11] It has been also reported that two isoprene units of ubiquinone could be modeled in the native structure of complex II by computational analysis using a protein-ligand docking program.[12] Napyradiomycin A1 is structurally similar to ubiquinone (Figure 1a); therefore, it is likely that napyradiomycin A1 binds with the ubiquinone-binding site of complexes I and II through its terpenoid residue. On the other hand, although mitochondrial complex III also includes a ubiquinone-binding site,[13] napyradiomycin A1 was unable to inhibit the activity of complex III up to 20 μM. Our result that napyradiomycin A1 inhibits mitochondrial complexes I and II but not complex III is interesting, because it has been reported that the structure of ubiquinone-binding sites in complex I and complex III may be similar, but they are different from a ubiquinone-binding site in complex II.[14] Further study is necessary to elucidate the mechanism by which napyradiomycin A1 inhibits mitochondrial complexes I and II but not complex III.

Isolation of napyradiomycins was first reported in 1986. Napyradiomycin group compounds were isolated from *Actinomycetes* and identified as antibacterial antibiotics.[3] At present, many napyradiomycins have been identified and reported to exhibit cytotoxicity against human cancer cell lines;[15] however, the molecular mechanism by which napyradiomycins show cytotoxicity has been unclear. Our results raise the possibility that an inhibitory effect of napyradiomycin A1 against the mitochondrial electron transport chain may explain the cytotoxicity of napyradiomycins against cancer cells.

ACKNOWLEDGEMENTS

This study was partly supported by a Grant-in-Aid for Scientific Research from the Ministry of Education, Culture, Sports, Science and Technology of Japan. This study was also supported by grants from Suzuken Memorial Foundation. This study was supported in part by the Global COE Program for Human Metabolomic Systems Biology of MEXT, Japan.

1 Kitagawa, M., Ikeda, S., Tashiro, E., Soga, T. & Imoto, M. Metabolomic identification of the target of the filopodia protrusion inhibitor glucopiericidin A. *Chem. Biol.* **17,** 989–998 (2010).
2 Motohashi, K., Sue, M., Furihata, K., Ito, S. & Seto, H. Terpenoids Produced by Actinomycetes: Napyradiomycins from Streptomyces antimycoticus NT17. *J. Nat. Prod.* **71,** 595–601 (2008).
3 Shiomi, K. *et al.* Novel antibiotics napyradiomycins. Production, isolation, physicochemical properties and biological activity. *J. Antibiot.* **39,** 487–493 (1986).
4 Pedersen, P L. *et al.* Preparation and characterization of mitochondria and submitochondrial particles of rat liver and liver-derived tissues. *Methods Cell Biol.* **20,** 411–481 (1978).
5 di Rago, J P. & Colson, A M. Molecular basis for resistance to antimycin and diuron, Q-cycle inhibitors acting at the Q_i site in the mitochondrial ubiquinol-cytochrome c reductase in *Saccharomyces cerevisiae*. *J. Biol. Chem.* **263,** 12564–12570 (1988).
6 Chance, B. The kinetics and inhibition of cytochrome components of the succinic oxidase system. III. Cytochrome b. *J. Biol. Chem.* **233,** 1223–1229 (1958).
7 Lenaz, G. *et al.* Coenzyme Q deficiency in mitochondria: kinetic saturation versus physical saturation. *Mol. Aspects Med.* **18**(Suppl), S25–31 (1997).
8 Chance, B., Williams, G R. & Hollunger, G. Inhibition of electron and energy transfer in mitochondria. I. Effects of Amytal, thiopental, rotenone, progesterone, and methylene glycol. *J. Biol. Chem.* **238,** 418–431 (1963).

9 Paddenberg, R. *et al.* Essential role of complex II of the respiratory chain in hypoxia-induced ROS generation in the pulmonary vasculature. *Am. J. Physiol. Lung Cell Mol. Physiol.* **284,** L710–719 (2003).
10 Rhein, V. *et al.* Amyloid-beta leads to impaired cellular respiration, energy production and mitochondrial electron chain complex activities in human neuroblastoma cells. *Cell Mol. Neurobiol.* **29,** 1063–1071 (2009).
11 Warncke, K. *et al.* Influence of hydrocarbon tail structure on quinone binding and electron-transfer performance at the Q_A and Q_B sites of the photosynthetic reaction center protein. *Biochemistry* **33,** 7830–7841 (1994).
12 Horsefield, R. *et al.* Structural and computational analysis of the quinone-binding site of complex II (succinate-ubiquinone oxidoreductase): a mechanism of electron transfer and proton conduction during ubiquinone reduction. *J. Biol. Chem.* **281,** 7309–7316 (2006).
13 Xia, D. *et al.* Crystal structure of the cytochrome bc_1 complex from bovine heart mitochondria. *Science* **277,** 60–66 (1997).
14 Tan, A. K., Ramsay, R. R., Singer, T. P. & Miyoshi, H. Comparison of the structures of the quinone-binding sites in beef heart mitochondria. *J. Biol. Chem.* **268,** 19328–19333 (1993).
15 Soria-Mercado, I. E., Prieto-Davo, A., Jensen, P. R. & Fenical, W. Antibiotic terpenoid chloro-dihydroquinones from a new marine actinomycete. *J. Nat. Prod.* **68,** 904–910 (2005).
16 Brusque, A. M. *et al.* Inhibition of the mitochondrial respiratory chain complex activities in rat cerebral cortex by methylmalonic acid. *Neurochem. Int.* **40,** 593–601 (2002).
17 Telford, J. E., Kilbride, S. M. & Davey, G. P. Decylubiquinone increases mitochondrial function in synaptosomes. *J. Biol. Chem.* **285,** 8639–8645 (2010).
18 Silveira, P. C., Streck, E. L. & Pinho, R. A. Evaluation of mitochondrial respiratory chain activity in wound healing by low-level laser therapy. *J. Photochem. Photobiol. B* **86,** 279–282 (2007).

Antitumor effects of novel highly hydrophilic and non-ATP-competitive MEK1/2 inhibitor, SMK-17

Masaki Kiga[a,c], Fumie Tanzawa[a], Shiho Iwasaki[a], Fumi Inaba[a], Kosaku Fujiwara[a], Hayato Iwadare[a], Tomoki Echigo[a], Yuji Nakamura[b], Tomoyuki Shibata[b], Kanae Suzuki[b], Isao Yasumatsu[a], Ayako Nakayama[c], Yukiko Sasazawa[c], Etsu Tashiro[c], Masaya Imoto[c] and Shinichi Kurakata[b]

The mitogen-activated protein kinase (MAPK) signal pathway plays a central role in regulating tumor cell proliferation, survival, and differentiation. The components of this pathway, Ras/Raf/MEK/ERK, are frequently activated in human cancers. Targeting this pathway is considered to be a promising anticancer strategy. In particular, MEK is an attractive drug target because of its high selectivity to ERK. We can expect potent growth inhibitory and proapoptotic effects by inhibiting MEK. Here, we report derivatives of *N*-[2-(2-chloro-4-iodo-phenylamino)-3,4-difluorophenyl]-methanesulfonamide as novel MEK1/2 inhibitors. Among these compounds, we found SMK-17 to be a potent MEK1/2 inhibitor with high aqueous solubility. The in-silico docking study suggested that SMK-17 is bound to an allosteric pocket of MEK1. The kinetic study and the kinase profiler analysis confirmed the allosteric nature of SMK-17. SMK-17 inhibited MEK1 kinase activity in a non-ATP-competitive manner and it was highly selective to MEK1 and 2. SMK-17 inhibited the growth of tumor cell lines *in vitro*. Especially, it seemed that cell lines harboring highly phosphorylated MEK1/2 and ERK1/2 were highly sensitive to SMK-17. Moreover, unlike previously reported MEK inhibitors, PD184352 or U0126, SMK-17 did not inhibit the phosphorylation of ERK5. *In vivo*, SMK-17 exhibited potent antitumor activity in animal models on oral administration. SMK-17 selectively blocked the MAPK pathway signaling without affecting other signal pathways, which resulted in significant antitumor efficacy without notable side effects. These findings suggest that SMK-17, an exquisitely selective, orally available MEK1/2 inhibitor, is a useful chemical biology tool for characterizing the function of MEK/MAPK signaling both *in vitro* and *in vivo*. *Anti-Cancer Drugs* 23:119–130 © 2011 Wolters Kluwer Health | Lippincott Williams & Wilkins.

Anti-Cancer Drugs 2012, 23:119–130

Keywords: allosteric inhibition, antitumor activities, cell cycle arrest, kinase inhibitor, xenograft model

[a]Kasai R&D Center, [b]Shinagawa R&D Center, Daiichi Sankyo Co. Ltd, Tokyo and [c]Department of Biosciences and Informatics, Faculty of Science and Technology, Keio University, Yokohama, Japan

Correspondence to Masaki Kiga and Kosaku Fujiwara, Kasai R&D Center, Daiichi Sankyo, Co. Ltd, 1-16-13, Kitakasai, Edogawa-ku, Tokyo 134-8630, Japan
Tel: +81 336 800 151; fax: +81 356 964 264;
e-mail: kiga.masaki.sm@daiichisankyo.co.jp and fujiwara.kosaku.t2@daiichisankyo.co.jp

Received 20 May 2011 **Revised form accepted** 27 August 2011

Introduction

The mitogen-activated protein kinases (MAPKs) are a family of serine/threonine protein kinases that play an important role in many cellular responses such as cell proliferation, survival, differentiation, movement, and apoptosis. The extracellular signal-regulated kinases 1 and 2 (ERK1/2) are the first characterized members of the MAPK family. ERK1/2 are activated by a phosphorylation cascade, downstream from the receptor tyrosine kinases, the ras protooncogene, Raf, and MEK1/2. Activated MEK1/2 catalyzes the phosphorylation of ERK1/2. These MAPKs phosphorylate a variety of substrates, including p90RSK and the transcription factor Elk-1, which mainly promote cell growth [1,2]. MEK1/2, also known as MKK1/2, are members of a large family of dual-specificity kinases (MKK1–7) that phosphorylate threonine and tyrosine residues of various MAPKs. Thus far, the only known substrates of MEK1/2 are ERK1/2. This tight selectivity indicates that MEK1/2 are essential for the MAPK pathway.

Constant activation of the MAPK pathway, because of aberrant receptor tyrosine kinase activation and Ras or BRAF mutations, is found frequently in human cancers and represents a major factor in determining abnormal cell growth [3]. Approximately 30% of all human cancers contain an activating Ras mutation. The incidence of K-ras mutations is particularly high in pancreatic and colon cancers (90 and 44%, respectively) [4]. Oncogenic V600E mutations in BRAF have been found in 66% of melanomas and 69% of papillary thyroid cancers [5,6]. Furthermore, aberrant activation of the MAPK pathway correlates with tumor progression and poor prognosis in patients with various cancers. Although active mutations of MEK1/2 have not been found in human cancers, the constitutive expression of MEK1/2 is sufficient to induce transformation [7,8]. Targeting MEK1/2 with a small

All supplementary digital content is available directly from the corresponding author.

0959-4973 © 2011 Wolters Kluwer Health | Lippincott Williams & Wilkins

DOI: 10.1097/CAD.0b013e32834c6a33

molecule inhibitor is an attractive strategy because of the potential to prevent all upstream aberrant oncogenic signaling [9,10]. Although previously reported MEK inhibitors, PD184352/CI-1040 and PD0325901, have been evaluated in a clinical study, these clinical trials were discontinued because of insufficient efficacy and undesirable adverse events [11–14]. ARRY142886/AZD6244 has been evaluated for clinical proof-of-concept in clinical trials. This compound has shown clinical responses in some patients with malignant melanoma and thyroid carcinoma [14,15]. However, no MEK inhibitors have been approved in the clinical use yet. More effective MEK inhibitors than previously reported compounds are needed for cancer therapy.

We report that SMK-17 is a hydrophilic, highly selective, and potent MEK1/2 inhibitor with a distinctively structured, piperidine sulfamide scaffold. SMK-17 exhibits significant antitumor activity *in vitro* and *in vivo* by selectively blocking the MAPK pathway signaling.

Materials and methods

Compounds

All compounds shown in Tables 1 and 2 were synthesized in-house, according to the procedure described in the patent application (WO2004083167).

Cell-free kinase assay

Homogeneous time-resolved fluorescence (HTRF) was used to detect MEK1/2 kinase activity. The reagents used in the assay are described below. Recombinant active human MEK1, MEK2, and GST-fused ERK2 were purchased from Millipore (Bedford, Massachusetts, USA). ATP was from Sigma-Aldrich Chemical (Saint Louis, Missouri, USA). Anti-phospho-ERK1/2 polyclonal antibody #9101 was from Cell Signaling Technology (Danvers, Massachusetts, USA). Polyclonal goat anti-rabbit antibody labeled with europium cryptate (PAR-K) and monoclonal anti-GST antibody labeled with XL665 (Mab GST-XL) were from Cisbio Bioassays (Bedford, Massachusetts, USA). In the presence or absence of testing compounds, the kinase reaction was conducted in 50 µl of reaction buffer [Tris (50 mmol/l), pH 7.4, $MgCl_2$ (10 mmol/l), EGTA (2 mmol/l), Na_3VO_4 (1 mmol/l), BSA (1 mg/ml)] containing 100 µmol/l ATP in a usual assay, 24 ng of active MEK1 or MEK2, and 100 ng of GST-fused ERK2 on a 96-well half-area EIA/RIA plate (Corning, New York, USA). After incubation at 30°C for 30 min, 25 µl of detection buffer [KF (1 mol/l), EDTA-PBS (50 mmol/l)], containing 1/500 diluted PAR-K, 1/1000 diluted antiphospho ERK1/2 polyclonal antibody, and 1/250 diluted MAb GST-XL, was added. After overnight incubation with a detection buffer, the phosphorylated ERK2 was measured with the Discovery HTRF microplate analyzer (PerkinElmer, Waltham, Massachusetts, USA). A ratio of 665 nm signal to 620 nm signal was regarded as the quantum of phosphorylation of ERK2. Values of wells that did not contain MEK were used as the baseline in each plate. IC_{50} (50% inhibitory concentration) values of MEK inhibition were calculated using the curve-fitting GraphPad Prism version 4 (GraphPad software, La Jolla, California, USA) from triplicate sets of data.

Table 1 Identification of a sulfamide compound as an MEK inhibitor

Compound		MEK1 kinase IC_{50} (nmol/l)	pERK in cell EC_{50} (nmol/l)	c Log $D_{7.4}$	Solubilities JP-1/JP-2 (nmol/l)
1	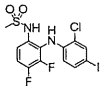	670	180	3.95	1.0/<0.5
PD184352	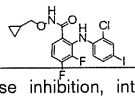	33	79	6.77	<0.5/<0.5

MEK1 kinase inhibition, intracellular MEK inhibition, *c*Log *D*, and aqueous solubility assay results of compound 1 and PD184352 as a reference compound.

Kinase selectivity

Kinase selectivity of SMK-17 at 1 µmol/l was tested against 233 human kinases by the Kinase Profiler (Millipore, *http://www.millipore.com/life_sciences/flx4/ld_kinases &tab1 = 3#tab1 = 3:tab2 = 1*).

Physicochemical study

JP-1 (aqueous acidic solution, pH 1.2) and JP-2 (neutral pH solution, pH 6.8) were purchased from Kanto Chemical (Tokyo, Japan). The sample solution was assayed using high-performance liquid chromatography (HPLC) methodologies. Two hundred and fifty micromoles per liter of the compound in aqueous CH_3CN solution [1 : 1 (v/v)] was prepared to make a calibration curve. The solubility was determined by comparing the ultraviolet peak area of the standard solution. The *c* Log *D* values were calculated by CLOGP software version 4.8.2 (Daylight Chemical Information Systems, Laguna Niguel, California, USA).

In-silico docking study

The molecular docking study was performed using Glide version 5.5 (Schrödinger, New York, New York, USA). The inhibitor was docked flexibly to an allosteric pocket adjacent to the ATP binding site of MEK1. The coordinates for the MEK1 were taken from a Protein Data Bank (PDBID: 3E8N [16]). In this structure, an allosteric inhibitor is bound adjacent to the ATP. The inhibitor molecule and water molecules that are unlikely to be important for ligand binding were deleted. Four structural water molecules that were bound to the magnesium ion or the side chain of A208 in the catalytic site, or the phosphates of the ATP, were preserved. After docking SMK-17 into the MEK1, energy minimization

Table 2 The structure–activity relationship of piperidine sulfamide scaffold for MEK inhibition and solubility screening

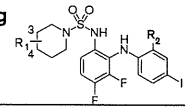

Piperidine series							
Compound	Substitution position	R1	R2	MEK1 kinase IC_{50} (nmol/l)	pERK in cell EC_{50} (nmol/l)	c Log $D_{7.4}$	Solubilities JP-1/JP-2 (nmol/l)
2	3-		Cl	40	360	3.42	-/-
3			F	42	770	−0.22	100/86
4			F	270	1500	−0.09	87/77
5			F	50	530	−0.41	91/88
6			F	34	110	−0.61	91/86
7	4-		Me	260	900	2.92	-/-
8			F	210	1500	2.45	12/21
9			Cl	210	400	3.39	-/-
10			Cl	180	300	3.68	1/2
11			Me	290	1800	−0.19	87/80
12			F	60	150	−0.65	92/84
13			Cl	92	52	0.73	88/74
14			Cl	74	800	0.63	89/61
15			Cl	72	190	0.71	-/-
16			F	33	220	−0.33	74/90
17 (SMK-17)			Cl	62	50	0.59	91/77
18			Cl	20	210	0.95	-/-
19			F	14	130	−0.31	86/78
20			F	41	430	−0.71	-/-
21			Cl	210	46	3.64	3/1

All tests were conducted by the same methods as in Table 1.

was performed on the complex with MacroModel version 9.7 (Schrödinger).

Cell culture

Colon 26 cells were provided by the Institute of Development, Aging, and Cancer, Tohoku University (Sendai, Japan). Other cell lines used in the experiments were purchased from American Type Culture Collection, and they were maintained with the recommended media supplemented with 10% heat-inactivated fetal bovine serum (HyClone Laboratories, Thermo Fisher Scientific, Waltham, Massachusetts, USA).

Western blot analysis

Anti-phospho-ERK (T202/Y204), anti-phospho-MEK (S217/221), anti-MEK1, anti-MEK2, anti-phospho-AKT (S473), anti-AKT, anti-cyclin D1, anti-phospho-S6 ribosomal protein (S235/236), anti-S6 ribosomal protein, anti-phospho-ERK5 (T218/Y220), anti-ERK5, anti-phospho-JNK (T183/Y185), anti-JNK, anti-phospho-p38 (T180/Y182), anti-p38α, anti-mouse HRP-linked IgG (#7076), and anti-rabbit HRP-linked IgG (#7074) were from Cell Signaling Technology. PhosphoSTOP; phosphatase inhibitor cocktail tablets and Complete Mini; and protease inhibitor cocktail tablets were from Roche Diagnostics (Indianapolis, Indiana, USA). Cells were seeded in six-well plates (Corning) 1 day before compound treatment. Then, the cells were treated with the compound for a specified period of time. Cells were harvested and lysed immediately with RIPA buffer (Tris HCl (50 mmol/l), pH 7.5, NaCl (150 mmol/l), Na_3VO_4 (1 mmol/l), 0.1% SDS, 0.5% deoxycholic acid, 1% IGEPAL CA-630, Phospho-

Fig. 1

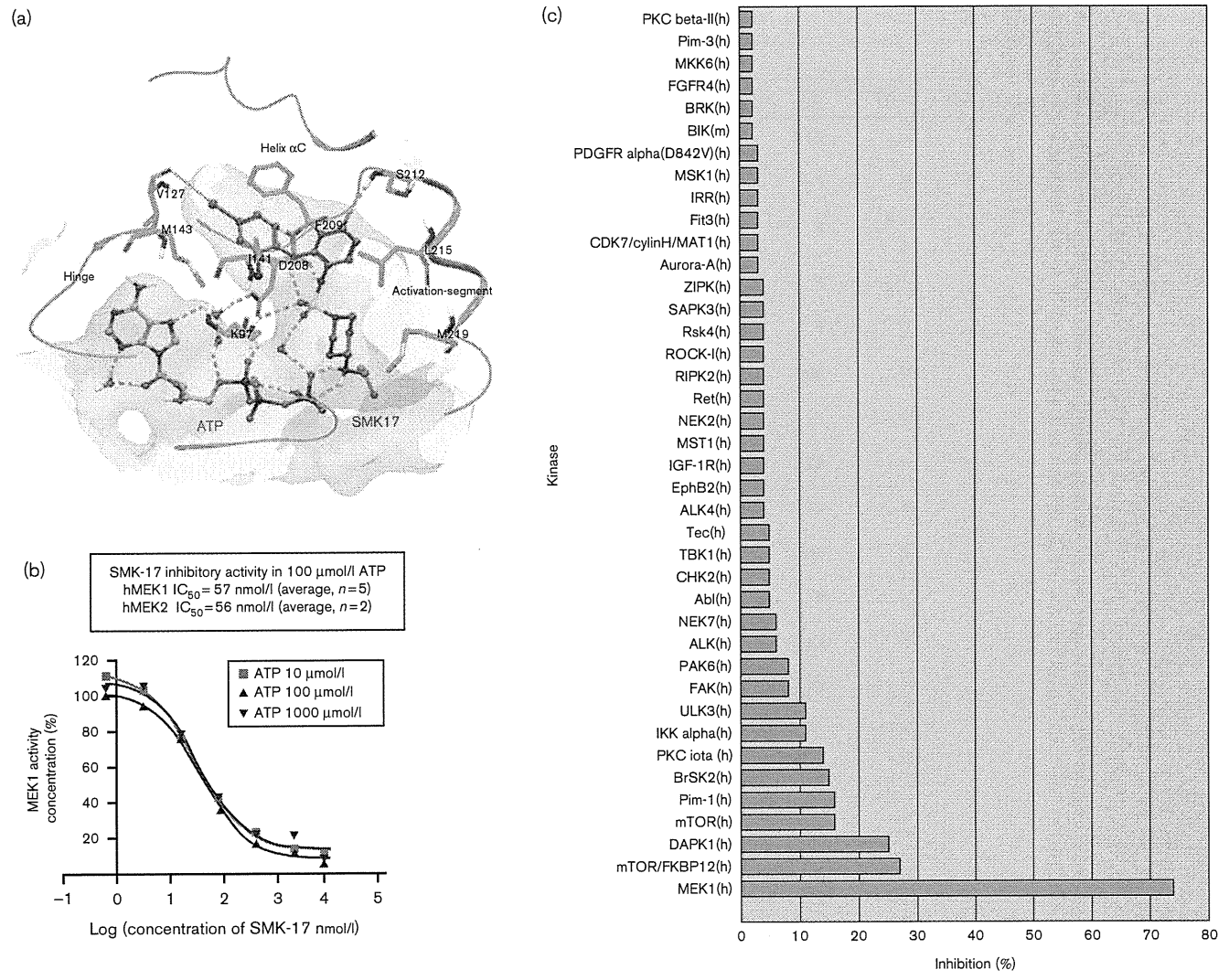

MEK1 kinase inhibition by SMK-17. (a) The predicted binding mode of SMK-17 with MEK1. View from the N-lobe. For simplicity, only important residues are shown. The hydrogen bondings and salt bridges are represented by cyan dotted lines. The MEK1 pocket surface is shown as a transparent gray surface. The figure was generated using Maestro version 9.0. (b) MEK kinase inhibition by SMK-17 at various ATP concentrations. Phosphorylation of ERK2 induced by MEK1 was detected by the homogeneous time-resolved fluorescence method. The IC_{50} value for MEK1 inhibition in this assay with 100 μmol/l of ATP was 37 nmol/l. The mean value of several independent experiments was 57 nmol/l for MEK1 kinase inhibition ($n=5$) and 56 nmol/l for MEK2 ($n=2$). (c) The Millipore Kinase Profiler data on 233 human kinases indicated that SMK-17 is a selective inhibitor against hMEK1 (1000 nmol/l, approximately 18-fold higher than IC_{50} for MEK1). The *x*-axis shows the percentage of inhibition against a specific kinase (*y*-axis). The top 40 kinases are shown in this figure.

STOP tablet, and Complete Mini tablet). Tumor tissues were harvested from mice and stored at −80°C and disrupted by grinding for 30 s at 2500 r.p.m. twice with a Multi-Beads Shocker (Yasui Kikai, Shizuoka, Japan) in the RIPA buffer. After incubation on ice for 30 min, the lysates were centrifuged at 14 000 *g* for 15 min to clear the insoluble fragments. The supernatants were used for western blot analysis. Equal amounts of total protein were resolved on SDS-PAGE gels and blotted with antibodies as indicated. The chemiluminescent signal was generated with Western Lightning Plus (PerkinElmer) and detected with a LAS-4000 imager (Fujifilm, Tokyo, Japan). The densitometric quantification of specific bands was performed using Multi Gauge Software (Fujifilm).

Cell enzyme-linked immunosorbent assay

NIH 3T3 cells were seeded at the appropriate density (1×10^5 cells/ml/well) on a 24-well flat-bottomed plate (Corning) and cultured for 24 h. The culture medium was changed to Dulbecco's Modified Eagle's Medium supplemented with 0.2% FBS. After 24 h incubation, the cells were treated with the compound for 1 h. Then,

Fig. 2

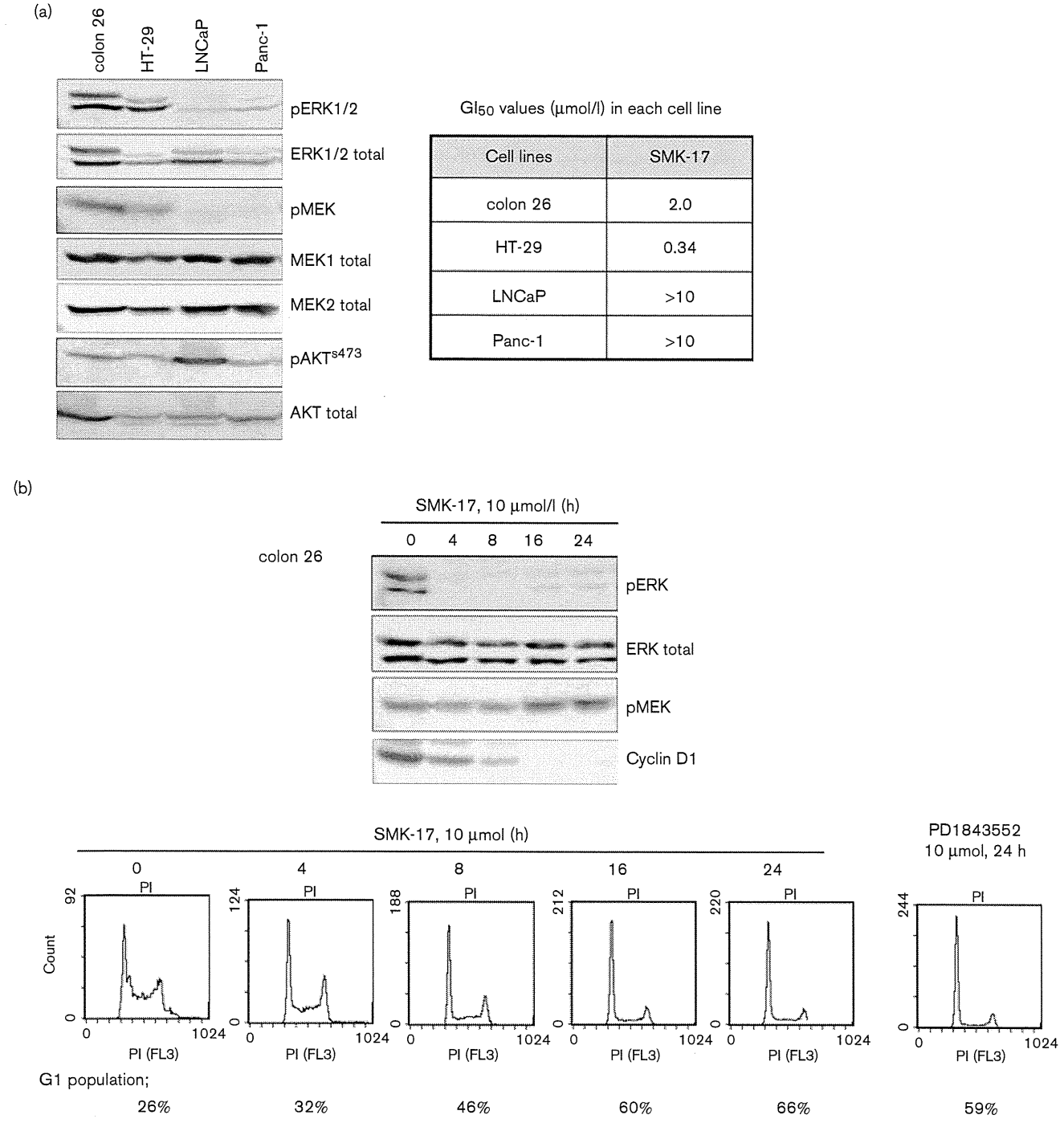

Growth inhibition profile of SMK-17. (a) Expression profile of MEK and ERK. Western blot analysis for pERK, ERK, pMEK, MEK1/2, pAKT^{S473}, and AKT. GI_{50} values of SMK-17 in a 72-h ATP assay are shown. (b–d) Effects of SMK-17 on the cell cycle and MEK/ERK pathway proteins in colon 26 (b), HT-29 (c), and Panc-1(d). SMK-17-induced and PD184352-induced G1 cell cycle arrest in colon 26 and HT-29 cells. Colon 26, HT-29, and Panc-1 cells were treated with SMK-17 (1, 10, or 30 μmol/l respectively; three-fold to five-fold of GI_{50} for each cell line) or PD184352 for 24 h and the cell cycle profiles were examined by flow cytometry analysis. The values for cell cycle distribution were derived using MultiCycle software. SMK-17 affects the expressions of proteins that are critical to G1 phase transition in the cell cycle. Cells were treated with SMK-17 for 24 h, and the cell lysates were analyzed by western blot using antibodies as indicated. (e) Dose correlation between MEK inhibition and cell cycle arrest on HT-29 cells. Phosphorylation and the total ERK expression after 24-h drug treatment were evaluated with a western blot. The G1 phase population was examined by flow cytometry analysis.

Fig. 2 (continued)

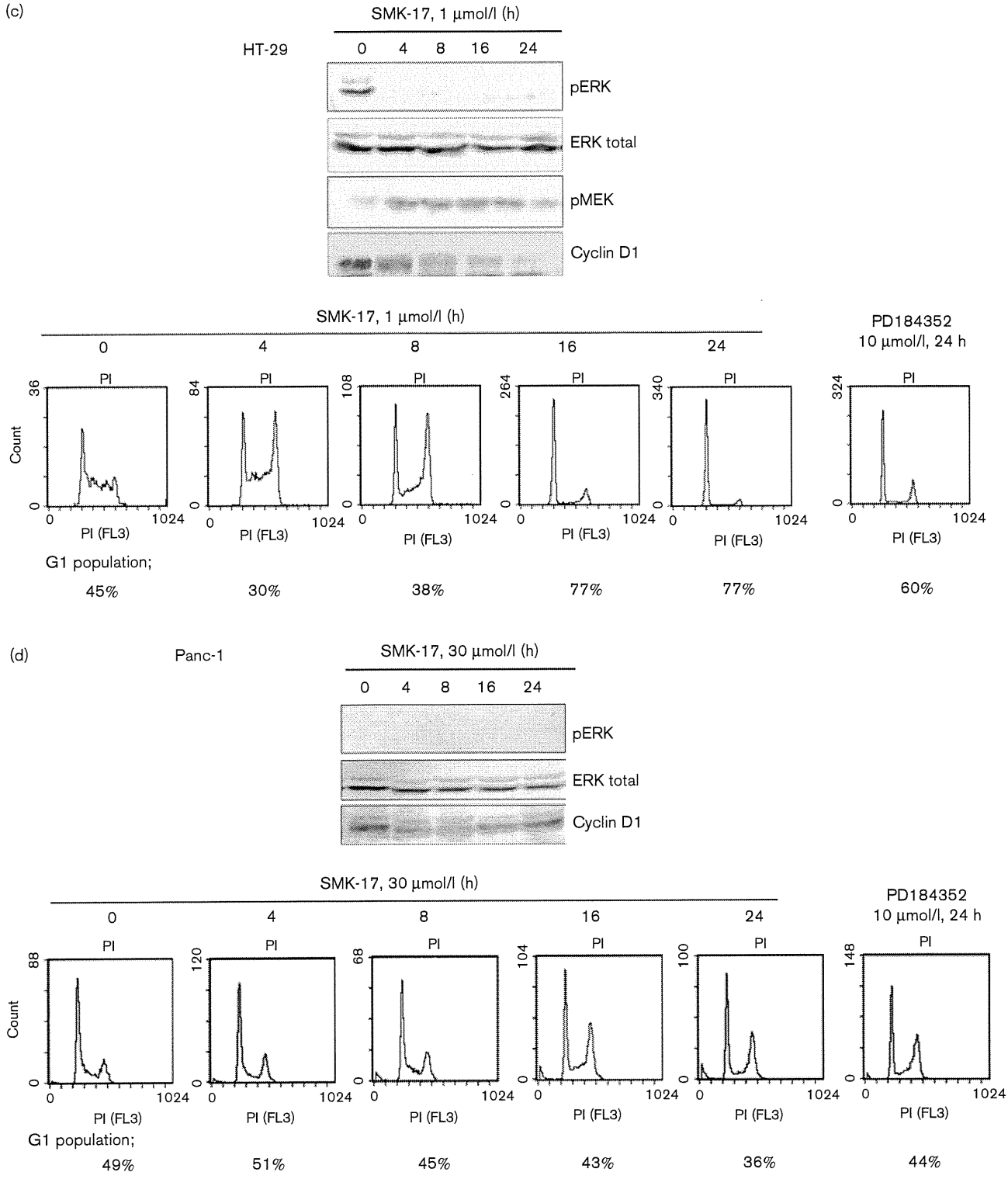

Fig. 2 (continued)

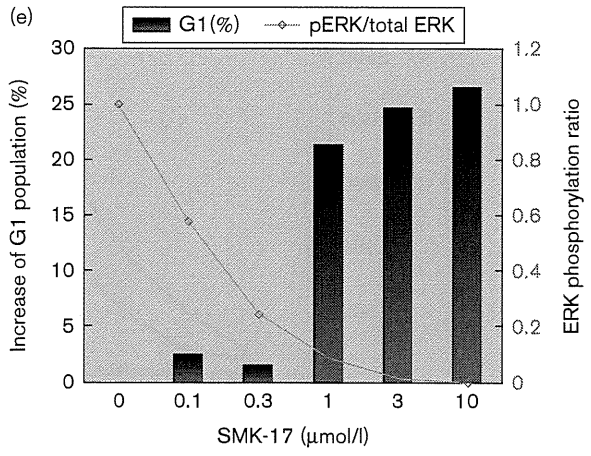

the cells were stimulated with an epidermal growth factor (EGF; Calbiochem, Merck KGaA, Darmstadt, Germany, final concentration 10 ng/ml) for 5 min. The cells were washed with cold PBS containing Na_3VO_4 (1 mmol/l) and fixed with −20°C methanol for 5 min. The cells were treated with blocking buffer (1% BSA, 0.05% Tween20-PBS) for 1 h, and incubated with primary antibodies for 2 h at 4°C. After being washed with 0.05%-Tween20-PBS twice, HRP-linked secondary antibodies in 1/1000 dilution was added and incubated at 4°C for 1 h. The cells were then washed three times and the detection substrate was added (OPD coloring reaction kit from Sumitomo Bakelite, Tokyo, Japan). The absorbance at 490 nm was then measured with a microplate reader (Model 3550, Bio-Rad Laboratories, Hercules, California, USA). In this experiment, EC_{50} values of MEK inhibition were calculated using the linear regression method. Two concentrations of each compound, which yielded MEK inhibitions closest to 50%, were chosen to calculate the EC_{50} values.

Cell growth inhibition assays

For growth inhibition experiments, cells were plated in black 96-well plates (Corning) at 1000 cells/100 μl/well. After 24-h culture, the compound was added and incubated for another 72 h. The cell number was measured using CellTiter-Glo (Promega, Fitchburg, Wisconsin, USA). Nonlinear curve fitting was performed using GraphPad Prism 4 from triplicate sets of data.

Cell cycle measurement

The percentage of cells in different cell cycle phases of division was measured by flow cytometry using propidium iodide (PI, Sigma-Aldrich) staining of cells [17]. In brief, tumor cells were treated with SMK-17 for the indicated time, fixed with 70% ethanol at −20°C, and then stained with PI (40 μg/ml) and RNase A (0.5 mg/ml) (Wako Pure Chemical Industries, Osaka, Japan) at 37°C for 30 min. PI fluorescence was measured with an EPICS XL Flow Cytometer (Beckman Coulter, Brea, California, USA) and analyzed using MultiCycle software (Phoenix Flow Systems, San Diego, California, USA)

Pharmacokinetic studies

SMK-17 was dosed by oral gavage to tumor-bearing mice. Three mice of each group were sacrificed after dosing, and plasma samples were collected and frozen at −20°C until analysis.

Acetonitrile deproteinized the plasma samples with a two-fold volume of the sample. The supernatant was obtained by centrifugation at 15 000*g* for 3 min at 4°C. Plasma concentrations of SMK-17 were determined by high-performance liquid chromatography analysis with ultraviolet detection at 280 nm. The mobile phase of HPLC was 0.5% phosphoric acid/acetonitrile (57/43, v/v) and the flow-rate was 1 ml/min through a YMC-Pack ODS-A column (A-312, 150 × 6.0 mm I.D., S-5 μm, YMC, Kyoto, Japan).

In-vivo antitumor study

Specific pathogen-free female nude mice (BALB/cA Jcl-nu) were purchased from CLEA Japan (Tokyo, Japan). Female CDF1 mice were from Charles River Japan (Yokohama, Japan). SMK-17 and PD184352 were suspended in 0.5% methyl cellulose solution (Wako Pure Chemical Industries), and administered daily to the animals by gavage (0.1 ml/10 g body weight). Control animals received 0.5% methyl cellulose solution for vehicle control. For the HT-29 study, 2×10^6 tumor cells were inoculated subcutaneously into the axillar region of the nude mice on Day 0. Tumor-bearing nude mice were grouped, and administration of SMK-17 or PD184352 was started on Day 3. For the colon 26 study, 2×10^5 cells were inoculated subcutaneously into CDF1 mice on Day 0. Tumor-bearing mice were grouped, and drug treatment was started on Day 3. Tumor volumes were calculated using a microgauge (Mitsutoyo, Kawasaki, Japan) according to the following equation: Tumor volume $(mm^3) = 1/2 \times (\text{tumor length}) \times (\text{tumor width})^2$.

Results and discussion

Potency of diphenyl amine sulfonamide derivatives as an MEK1/2 inhibitor

In this article, we describe the discovery of the new derivative series of diphenyl amine sulfonamide as potent MEK inhibitors. We summarize the optimization of the sulfonamide modification, which has culminated in the identification of the potent and highly water soluble MEK inhibitor, SMK-17 (compound 17 in Table 2). The goal of this study was to identify a compound that possessed potent antitumor activity *in vivo* with high oral availability, which required high aqueous solubility for oral absorption and a strong MEK-inhibiting activity. An HTRF-based kinase assay was used for the primary screening. Then, phospho-ERK-detecting cell enzyme-

Fig. 3

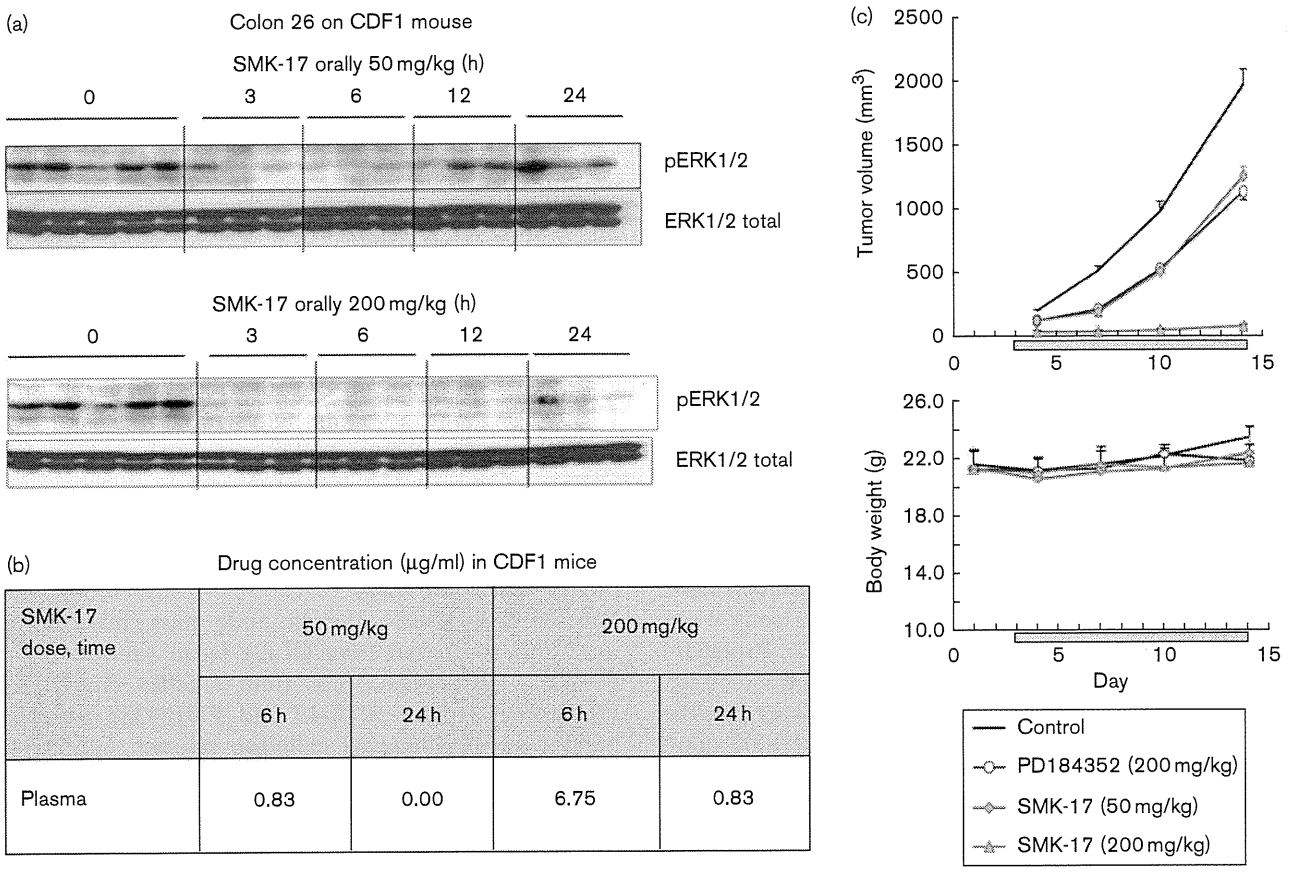

(b) Drug concentration (μg/ml) in CDF1 mice

SMK-17 dose, time	50 mg/kg		200 mg/kg	
	6 h	24 h	6 h	24 h
Plasma	0.83	0.00	6.75	0.83

The *in-vivo* efficacy of SMK-17. (a) After a single oral dose of SMK-17 to colon 26-CDF1 mice, tumors were excised at various time points after dosing, and the tumor lysates were analyzed by western blot. Administration of SMK-17 at 50 mg/kg achieved phospho-ERK1/2 inhibition in tumors for 6 h. Significant phospho-ERK1/2 inhibition was observed up to 24 h after dosing in mice treated with 200 mg/kg compared with the untreated controls. (b) SMK-17 concentration (μg/ml) in the plasma of the drug-treated CDF1 mice after administration. (c) SMK-17 exhibits significant in-vivo antitumor efficacy that correlates with its inhibition of MAPK signaling in colon26-CDF1 mice. (d) Western blot analysis of MAPKs and AKT signals in an HT-29 xenograft. (e) In-vivo antitumor activity of SMK-17 on HT-29 xenograft.

linked immunosorbent assay was used to measure the intracellular MEK activity. The oral absorption of each compound was predicted by calculating the lipophilicity ($c\,\mathrm{Log}\,D$) and aqueous solubility.

We identified a novel compound, *N*-[2-(2-chloro-4-iodo-phenylamino)-3,4-difluorophenyl]-methanesulfonamide (compound 1 in Table 1), as an MEK inhibitor in the above-described screening. It has a sulfamide substituent that is different from previously reported MEK inhibitors such as U0126, PD98059, and PD184352. This compound showed weak activity in in-vitro assays and poor water solubility: less than 0.5 μmol/l of solubility in pH 6.8 solution. We adopted compound 1 as the starting compound and tried to obtain derivatives with improved potency and aqueous solubility for the development of an orally absorbable potent MEK inhibitor.

As the first step of modification of the starting compound, we added the sulfonamide of compound 1 to the hydroxy-piperidine-group. As a result, compounds 2 and 9 in Table 2 showed 17-fold and three-fold increases in MEK1 kinase inhibition compared with compound 1. As the second step, the terminal piperidine-sulfamide was added to various polar substituents to demonstrate the structure–activity relationship of this substructure. The structure–activity relationship was established with two varying positions (R1 and R2 in Table 2). The activities of the piperidine-sulfamide series indicated that a substituent for the chlorine group was desired at the R2 position in cell-based potency rather than for the fluorine or methyl groups, as evidenced by compounds 7–9, 11–13, 16, and SMK-17. The cell-free activities of compounds including fluorine at the R2 position (12 and 16) were more potent than those with a chlorine group (13 and SMK-17). This reversal of potency order between cell-free and cell-based activity is considered to be due to the cell membrane permeability of these compounds. In addition, an alkyl-amine substituent at the fourth (*para*)

Fig. 3 (continued)

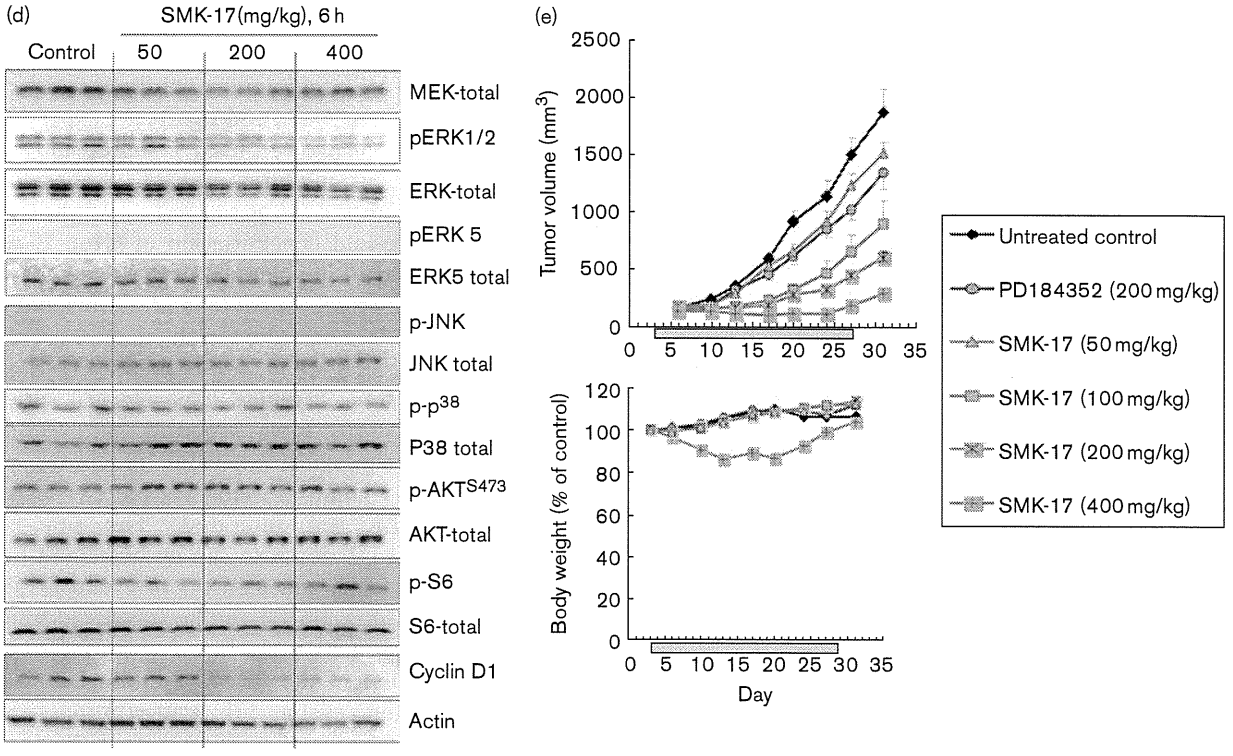

position of R1, which is adopted in compounds 11–19, was the favorable structure for both cell-free and cell-based MEK inhibition. In contrast, hydroxy-terminal substituents such as in compounds 2, 7–10, and 20 were unfavorable. In particular, an isopropyl-amine at the fourth position (SMK-17) was the optimal structure for both intracellular and cell-free MEK1 kinase inhibition.

A low *c*Log*D*, which predicts high water solubility, is required for in-vivo exposure of orally administered drugs. The *c*Log*D* of compound 1 is 3.95 and the solubility in JP-2 (pH 6.8) buffer is less than 0.5 μmol/l. Alkyl-amine-adopted derivatives (compounds 3–6, 11–19) achieved a lower *c*Log*D* and a higher water solubility in the range of 61–88 μmol/l in JP-2 solution, compared with the piperidinol series (compounds 2, 7–10), in addition to improvement in in-vitro activities. Adoption of a basic residue such as alkyl-amine in the R1 position is considered to contribute to the improvement of the polar nature and high aqueous solubility.

We observed two significant structure–activity relationships in the compound's optimization. First, substitution of alkyl-amine, especially an isopropyl-amine, at the R1 position yielded better profiles of both aqueous solubility and in-vitro activities. A comparison between the cell-based MEK inhibitory potencies of compound 9 and its isopropyl-amine analog (SMK-17) revealed an eight-fold improvement. The second critical finding was that a substituent for chlorine was desirable at the R2 position rather than for fluorine or methyl. Substitution of chlorine for fluorine at the R2 position of compound 16 results in a four-fold increase in the intracellular MEK inhibition of SMK-17. The same substitution in the piperidinol pair (analogs 8 and 9) provides an approximately three-fold improvement in cell potency. The two structure–activity relationships advance providing the benefit of improved aqueous solubility and in-vitro activity. We finally obtained SMK-17, which has a more than 100-fold aqueous solubility in JP-2 and 11-fold strengthened MEK kinase inhibition.

Binding mode to MEK1

To understand the characteristics of these derivatives, we built a docking model of SMK-17 and MEK1 (Fig. 1a). The predicted binding model showed that SMK-17 binds to an allosteric pocket adjacent to the ATP-binding site similar to U0126 or PD325089 [18], which indicates that SMK-17 is a non-ATP-competitive inhibitor. In addition, the protonated amine of the alkyl-amine group at the R1 forms salt bridges with the γ phosphate of ATP. The aliphatic carbons of the alkyl-amine substituent have hydrophobic interactions with M219 and V224 (not shown in this figure) in the activation segment. This predicted binding mode supports the structure–activity relationship that inhibitory activity is well correlated with the size of the alkyl-amine as shown in Table 2.

ATP dependency of kinase inhibition

To confirm the allosteric binding characteristic of SMK-17 predicted in Fig. 1a, we examined the ATP dependence of MEK1 inhibition by SMK-17 and tested MEK1 kinase inhibition at various concentrations of ATP from 10 to 1000 μmol/l (Fig. 1b). The ATP concentration was found to have little effect on the MEK1 inhibition of SMK-17. IC_{50} values of SMK-17 for MEK1 kinase were 31.4 (ATP 10 μmol/l), 36.6 (100 μmol/l), and 36.5 nmol/l (1000 μmol/l) respectively. Thus, SMK-17 was regarded as a non-ATP-competitive inhibitor of MEK1. These results coincide with the prediction by the in-silico binding model that SMK-17 does not exclude ATP from MEK1.

Kinase inhibitory selectivity

SMK-17 was further characterized for its kinase selectivity with Millipore's kinase profiler. The screen of 233 protein kinases incubated with 1000 nmol/l of this compound has been described in Supplement 4. Figure 1c shows the top 40 kinases, which were inhibited by SMK-17. MEK1 was the kinase most sensitive to SMK-17, and was inhibited by 74%. There was no significant (> 50%) inhibition of any other protein kinases observed except for MEK1. Notably, SMK-17 had little effect on MEK1 isoforms, such as MKK4 (29% inhibition), MKK6 (2%), and MKK7 (32%). The non-ATP-competitive but allosteric binding mode of this compound probably contributes to its high selectivity to MEK1/2.

Despite their allosteric inhibition mode, PD184352 and U0126 were previously reported to inhibit MKK5 as an off-target [19]. It is supposed that the conformation of the allosteric pocket of MEK1/2 is similar to that of MKK5. However, SMK-17 did not inhibit ERK5 phosphorylation, which is a substrate of MKK5 in both cell-based and in-vivo experiments (Fig. 3d and Supplement 1). These results indicated that SMK-17 is a non-ATP-competitive and highly selective kinase inhibitor of MEK1/2.

Intracellular MEK and growth inhibition

To further investigate the intracellular effects of SMK-17, the antiproliferative effect of SMK-17 was examined against murine colorectal cancer colon 26, human colorectal cancer HT-29, human pancreas cancer Panc-1, and human prostate cancer LNCaP. SMK-17 was active in suppressing cell growth in colon 26 and HT-29 cell lines, which harbor highly phosphorylated MEK1/2 and ERK1/2. The GI_{50} values were 2.0 and 0.34 μmol/l, respectively (Fig. 2a). In contrast, SMK-17 was not effective in tumor cells, which do not have highly phosphorylated MEK1/2 and ERK1/2, such as Panc-1 and LNCaP cells. As reported previously with the other MEK inhibitors [20], SMK-17 is highly effective in suppressing the proliferation of tumor cells with aberrant activated MAPK pathway signaling, which is reflected by the phosphorylation levels of MEK1/2 and ERK1/2.

To understand the underlying mechanism of SMK-17 activity on cancer cell proliferation, we analyzed its effect on the cell cycle progression and cyclin D1 expression in tumor cells. In responsive cell lines, colon 26 and HT-29 colorectal cancer cells, inhibition of ERK1/2 phosphorylation by SMK-17 led to a G1 phase cell cycle arrest at an approximately five-fold concentration of GI_{50}, 10 μmol/l in HT-29 and 1 μmol/l in colon 26 (Fig. 2b and c), which were similar to the effects of PD184352. Correspondingly, treatment with SMK-17 resulted in the downregulation of cyclin D1, a key cell cycle regulator for G1–S phase progression, which is a typical physiological effect of MEK1/2 inhibitors [10]. It was reported that cyclin D1 is an unstable protein, with a half-life of approximately 30 min [21]. The amount of cyclin D1 protein decreased 8–16 h after MEK was inhibited. The time-lagged response of cyclin D1 decrease can be explained by two independent regulatory mechanisms of cyclin D1. First, protein synthesis of cyclin D1 can be translated from the remaining mRNA. The translation of cyclin D1 does not stop briefly, although the MEK inhibitor suppresses MEK-ERK-inducing cyclin D1 transcription activity. Second, phosphorylation of cyclin D1 at T286 by ERK enhances its ubiquitination and proteasomal degradation [22]. Hence, inhibition of MEK-ERK attenuates the phosphorylation of T286 and the degradation of cyclin D1 protein. Accordingly, inhibition of MEK-ERK results in a slow decrease in cyclin D1. A negative feedback mechanism by ERK, which suppresses upstream of the ras/raf signal pathway, has been reported in the previous study [23]. In this report, we observed an increased phosphorylation of MEK by SMK-17 in HT-29 cells. As the MEK inhibitor suppressed the activity of ERK including the negative feedback pathway, SMK-17 was likely to cause increased MEK1/2 phosphorylation by inactivating the negative feedback mechanism.

In contrast, in resistant Panc-1 and LNCaP cells, SMK-17 at the concentration of 30 μmol/l did not lead to marked G1 phase arrest and downregulation of cyclin D1 (Fig. 2d and Supplement 5). It is possible that proliferation of resistant cell lines is independent of MEK/MAPK pathway because these cell lines have phosphorylated S473 of AKT, which represents PI3K/AKT pathway activation (Fig. 2a). PI3K-dependent growth of Panc-1 cells are supported by several reports [24–26]. Our results support the PI3K pathway-dependent growth of MEK inhibitor-resistant cell lines. Furthermore, SMK-17 did not induce apoptosis, as evidenced by the sub-G1 population on flow cytometry analysis in all four cell lines, even under conditions of complete MEK inhibition (e.g. 10 μmol/l of SMK-17 on HT-29 cells). We confirmed that SMK-17 did not induce apoptosis in these cell lines, which were monitored with AnnexinV-APC and 7AAD double staining (data not shown). These results indicated that inhibition

of MEK/ERK signal pathway is not sufficient to induce apoptosis in all four cell lines.

To examine whether MEK inhibition of SMK-17 affects cell cycle arrest directly, we investigated the dose correlation between cell cycle arrest and intracellular MEK inhibition. As a result, an inverse correlation was observed between the intensity of ERK phosphorylation and an increase in the G1 population (Fig. 2e). Moreover, SMK-17 selectively inhibited Raf/MEK/ERK pathway activity in cells while having no effect on the activation status of other closely related intracellular signaling molecules such as ERK5, p38, JNK, and AKT (Supplement 1). These results indicated that SMK-17 induced G1 arrest through intracellular MEK1/2 inhibition as an on-target effect.

In-vivo antitumor activity

We evaluated the in-vivo efficacy of SMK-17 using the murine colorectal colon 26 cell syngeneic model in CDF1 mice. Colon 26 cells have a constitutively active K-ras mutation. After a single oral dose of SMK-17, tumors were excised at various time points after dosing and the tumor lysates were analyzed for phospho-ERK1/2 and total ERK levels. SMK-17 decreased the phospho-ERK1/2 level in the tumor mass after 50 mg/kg administration for 6 h. Treatment using 200 mg/kg caused a 24-h inhibition of phospho-ERK1/2 (Fig. 3a and Supplement 2 as quantification data).

The antitumor activity of SMK-17 was evaluated in the same model in CDF1 mice. When SMK-17 was administered to mice once daily at doses of 50 and 200 mg/kg, the antitumor activity was observed, from partial tumor growth inhibition at doses of 50 mg/kg to complete inhibition at 200 mg/kg (Fig. 3c) without significant body weight loss. In this experiment, PD184352 as a reference also showed tumor growth inhibition. In this syngeneic graft model, blood samples were collected from animals and the drug concentration in the plasma was measured for pharmacokinetic and pharmacodynamic analyses. SMK-17 concentrations in the plasma of mice are shown in Fig. 3b. Complete inhibition of ERK phosphorylation in tumors was achieved when the plasma drug concentration was more than 0.83 μg/ml (comparable to 1.4 μmol/l, $M_w = 584.8$). This minimum effective plasma concentration is similar to the GI_{50} value of colon 26 cells *in vitro*. Administration of 200 mg/kg of SMK-17, at which complete inhibition of intratumor MEK for 24 h per dosing occurs, caused complete inhibition of tumor growth. These results indicated that continuous exposure of SMK-17 was necessary for long-lasting inhibition of intratumor MEK1/2 and complete tumor growth inhibition in an animal model.

Furthermore, we evaluated the in-vivo pharmacodynamic study on SMK-17 against the HT-29 human tumor xenograft model (Fig. 3d). In this model, SMK-17 showed a dose-dependent phospho-ERK inhibition and cyclin D1 reduction in tumors 6 h after administration, similar to in-vitro results. Figure 3d shows that significant effects on the other signals except for ERK1/2 were not observed up to 400 mg/kg (e.g. phosphorylation S473 of AKT, S6, and the other MAPKs). It is suggested that SMK-17 selectively inhibited Raf/MEK/ERK pathway activity in the xenograft model. Exposure of SMK-17 in this animal model was similar to that in the colon 26 CDF1 mice model (Supplement 3). No difference in pharmacokinetics between nude mice and CDF1 mice was observed. We evaluated the antitumor activity of SMK-17 against this xenograft model. SMK-17 was orally administered daily at a dose range of 50–400 mg/kg in tumor-bearing mice for 25 days and it showed statistically significant tumor growth inhibition in a dose-dependent manner (Fig. 3e). In this study, partial tumor growth inhibition was observed at doses between 50 and 200 mg/kg, and complete inhibition was observed at 400 mg/kg. No notable adverse effects were observed in this study.

Conclusion

In conclusion, we found a very potent MEK inhibitor, SMK-17, from our structure–activity correlation study of the new derivative series of diphenyl amine sulfonamides. Kinase profiler and kinetic studies revealed that SMK-17 is a non-ATP-competitive and highly selective MEK1/2 inhibitor. Moreover, SMK-17 exhibited potent antitumor activity in animal models by oral administration. SMK-17 selectively blocked the MAPK pathway signaling without affecting other signal pathways both *in vitro* and *in vivo*. These findings suggest that SMK-17 is a useful chemical biology tool for characterizing the function of MEK/MAPK signaling both *in vitro* and *in vivo*.

Acknowledgements

We would like to thank Dr Kenichi Wakita for critical reading of the manuscript. We would also like to thank Dr Tohru Takashi and Dr Koichi Akahane for continuous encouragement in conducting these studies.

Conflicts of interest

There are no conflicts of interest.

References

1 Dalby KN, Morrice N, Caudwell FB, Avruch J, Cohen P. Identification of regulatory phosphorylation sites in mitogen-activated protein kinase (MAPK)-activated protein kinase-1a/p90rsk that are inducible by MAPK. *J Biol Chem* 1998; **273**:1496–1505. *http://www.ncbi.nlm.nih.gov/pubmed/9430688.*

2 Marais R, Wynne J, Treisman R. The SRF accessory protein Elk-1 contains a growth factor-regulated transcriptional activation domain. *Cell* 1993; **73**:381–393. *http://www.ncbi.nlm.nih.gov/pubmed/8386592.*

3 Sebolt-Leopold JS, Herrera R. Targeting the mitogen-activated protein kinase cascade to treat cancer. *Nat Rev Cancer* 2004; **12**:937–947. *http://www.ncbi.nlm.nih.gov/pubmed/15573115, http://www.nature.com/nrc/journal/v4/n12/full/nrc1503.html.*

4 Bos JL. Ras oncogenes in human cancer. *Cancer Res* 1990; **50**:1352. *http://www.ncbi.nlm.nih.gov/pubmed/2547513, http://cancerres.aacrjournals.*

org/content/49/17/4682.abstract?ijkey=332fc8fd82a5e0c5b13dc693262953e7ccddd4f1&keytype2=tf_ipsecsha.

5 Davies H, Bignell GR, Cox C, Stephens P, Edkins S, Futreal PA, *et al.* Mutations of the BRAF gene in human cancer. *Nature* 2002; **417**:949–954. *http://www.ncbi.nlm.nih.gov/pubmed/12068308?dopt=Abstract.*

6 Cohen Y, Xing M, Mambo E, Guo Z, Wu G, Sidransky D, *et al.* BRAF mutation in papillary thyroid carcinoma. *J Natl Cancer Inst* 2003; **95**:625–627. *http://www.ncbi.nlm.nih.gov/pubmed/12697856 http://jnci.oxfordjournals.org/content/95/8/625.abstract?ijkey=da94f758df955accebe5e60e4aa34896bf2dae22&keytype2=tf_ipsecsha.*

7 Cowley S, Paterson H, Kemp P, Marshall CJ. Activation of MAP kinase kinase is necessary and sufficient for PC12 differentiation and for transformation of NIH 3T3 cells. *Cell* 1994; **77**:841–852. *http://www.cell.com/retrieve/pii/0092867494901333.*

8 Mansour SJ, Matten WT, Hermann AS, Candia JM, Rong S, Ahn NG, *et al.* Transformation of mammalian cells by constitutively active MAP kinase kinase. *Science* 1994; **265**:966–970. *http://www.ncbi.nlm.nih.gov/pubmed/8052857, http://www.sciencemag.org/content/265/5174/966.abstract?ijkey=d4d45ca3cd0ae4da25d4d2391f3db8d265c7732f&keytype2=tf_ipsecsha.*

9 Sebolt-Leopold JS. MEK inhibitors: a therapeutic approach to targeting the Ras-MAP kinase pathway in tumors. *Curr Pharm Des* 2004; **10**: 1907–1914. *http://www.ncbi.nlm.nih.gov/pubmed/15180527.*

10 Roberts PJ, Der CJ. Targeting the Raf-MEK-ERK mitogen-activated protein kinase cascade for the treatment of cancer. *Oncogene* 2007; **26**:3291–3310. *http://www.nature.com/onc/journal/v26/n22/full/1210422a.html.*

11 Chiappori AA, Ellis PM, Hamm JT, Bitran JD, Eiseman I, Zinner RG, *et al.* Multicenter phase II study of the oral MEK inhibitor, CI-1040, in patients with advanced non-small-cell lung, breast, colon, and pancreatic cancer. *J Clin Oncol* 2004; **22**:4456–4462. *http://www.ncbi.nlm.nih.gov/pubmed/15483017.*

12 Lorusso P, Krishnamurthi S, Rinehart JR, Nabell L, Croghan G, Meyer MB, *et al.* A phase 1-2 clinical study of a second generation oral MEK inhibitor, PD 0325901 in patients with advanced cancer. *J Clin Oncol* 2005; **23**:3006. *http://meeting.ascopubs.org/cgi/content/abstract/23/16_suppl/3011.*

13 LoRusso P, Krishnamurthi S, Rinehart J, Nabell L, Croghan G, Wilner K, *et al.* Clinical aspects of a phase I study of PD-0325901, a selective oral MEK inhibitor, in patients with advanced cancer. *Mol Cancer Ther* 2007; **6**:3649s. (abstract B113). *http://www.sciencedirect.com/science?_ob=ArticleURL&_udi=B6T54-4VKMWBS-4&_user=937415&_coverDate=10%2F08%2F2009&_rdoc=1&_fmt=high&_orig=gateway&_origin=gateway&_sort=d&_docanchor=&view=c&_searchStrId=1694032765&_rerunOrigin=google&_acct=C000048659&_version=1&_urlVersion=0&_userid=937415&md5=d8112eaf600851f6b09b690d5a452dc1&searchtype=a.*

14 Thomson Pharma's HP; *www.thomson-pharma.com.*

15 Adjei AA, Cohen RB, Franklin W, Morris C, Wilson D, Eckhardt SG, *et al.* Phase I pharmacokinetic and pharmacodynamic study of the oral, small-molecule mitogen-activated protein kinase kinase 1/2 inhibitor AZD6244 (ARRY-142886) in patients with advanced cancers. *J Clin Oncol* 2008; **26**:2139–2146. *http://jco.ascopubs.org/content/26/13/2139.abstract?ijkey=86693f9a25dc33babae4808e1f2ca817d9adf20d&keytype2=tf_ipsecsha.*

16 Iverson C, Larson G, Lai C, Yeh LT, Dadson C, Quart B, *et al.* RDEA119/BAY 869766: a potent, selective, allosteric inhibitor of MEK1/2 for the treatment of cancer. *Cancer Res* 2009; **69**:6839–6847. *http://www.ncbi.nlm.nih.gov/pubmed/19706763.*

17 Darzynkiewicz Z, Li X. Measurements of cell death by flow cytometry. In: Cotter TG, Martin SJ, editors. *Techniques in apoptosis: a users' guide.* London: Portland Press. 1996; pp. 71–106.

18 Fischmann TO, Smith CK, Mayhood TW, Myers JE, Reichert P, Madison VS, *et al.* Crystal structures of MEK1 binary and ternary complexes with nucleotides and inhibitors. *Biochemistry* 2009; **48**:2661–2674. *http://pubs.acs.org/doi/abs/10.1021/bi801898e http://www.ncbi.nlm.nih.gov/pubmed/19161339.*

19 Mody N, Leitch J, Armstrong C, Dixon J, Cohen P. Effects of MAP kinase cascade inhibitors on the MKK5/ERK5 pathway. *FEBS Lett* 2001; **502**: 21–24. *http://www.ncbi.nlm.nih.gov/pubmed/11478941.*

20 Daouti S, Wang H, Li WH, Higgins B, Kolinsky K, Niu H, *et al.* Characterization of a novel mitogen-activated protein kinase kinase 1/2 inhibitor with a unique mechanism of action for cancer therapy. *Cancer Res* 2009; **69**:1924–1932. *http://www.ncbi.nlm.nih.gov/pubmed/19244124.*

21 Guo Y, Stacey DW, Hitomi M. Post-transcriptional regulation of cyclin D1 expression during G2 phase. *Oncogene* 2002; **21**:7545–7556. *http://www.nature.com/onc/journal/v21/n49/abs/1205907a.html, http://www.ncbi.nlm.nih.gov/pubmed?term=Oncogene%20(2002)%2021%2C%207545%20%E2%80%93%207556.*

22 Shao J, Sheng H, DuBois RN, Beauchamp RD. Oncogenic ras-mediated cell growth arrest and apoptosis are associated with increased ubiquitin-dependent Cyclin D1. *J Biol Chem* 2000; **275**:22916–22924. *http://www.jbc.org/content/275/30/22916.abstract, http://www.ncbi.nlm.nih.gov/pubmed?term=Oncogenic%20Ras-mediated%20Cell%20Growth%20Arrest%20and%20Apoptosis%20are%20Associated%20with%20Increased%20Ubiquitin-dependent%20Cyclin%20D1.*

23 Dougherty MK, Müller J, Ritt DA, Zhou M, Zhou XZ, Morrison DK, *et al.* Regulation of Raf-1 by direct feedback phosphorylation. *Mol Cell* 2005; **17**:215–224. *http://www.ncbi.nlm.nih.gov/pubmed/15664191.*

24 Yao Z, Okabayashi Y, Yutsudo Y, Kitamura T, Ogawa W, Kasuga M. Role of Akt in growth and survival of PANC-1 pancreatic cancer cells. *Pancreas* 2002; **24**:42–46. *http://www.ncbi.nlm.nih.gov/pubmed/11741181.*

25 Takeda A, Osaki M, Adachi K, Honjo S, Ito H. Role of the phosphatidylinositol 3kinase–Akt signal pathway in the proliferation of human pancreatic ductal carcinoma cell lines. *Pancreas* 2004; **28**: 353–358. *http://www.ncbi.nlm.nih.gov/pubmed/15084985.*

26 Perugini RA, McDade TP, Vittimberga FJ Jr, Callery MP. Pancreatic cancer cell proliferation is phosphatidylinositol 3-kinase dependent. *J Surg Res* 2000; **90**:39–44. *http://www.ncbi.nlm.nih.gov/pubmed/10781373.*

Bioorganic & Medicinal Chemistry 20 (2012) 1910–1921

Contents lists available at SciVerse ScienceDirect

Bioorganic & Medicinal Chemistry

journal homepage: www.elsevier.com/locate/bmc

Target identification of bioactive compounds

Etsu Tashiro, Masaya Imoto *

Department of Biosciences and Informatics, Faculty of Science and Technology, Keio University, 3-14-1 Hiyoshi, Kohokuku, Yokohama, Kanagawa 223-8522, Japan

ARTICLE INFO

Article history:
Available online 4 November 2011

Keywords:
Target identification
Bioactive compounds
Protein function
Chemical genetics

ABSTRACT

To fully understand the regulation of cellular events, functional analysis of each protein involved in the regulatory systems is required. Among a variety of methods to uncover protein function, chemical genetics is a remarkable approach in which small molecular compounds are used as probes to elucidate protein functions within signaling pathways. However, identifying the target of small molecular bioactive compounds isolated by cell-based assays represents a crucial hurdle that must be overcome before chemical genetic studies can commence. A variety of methods and technologies for identifying target proteins have been reported. This review therefore aims to describe approaches for identifying these molecular targets.

1. Introduction

To improve our understanding of complex cell systems, functional analysis of proteins has become a significant focus for a growing number of research fields in biology in the post-genome era.[1] Proteins play an intrinsic role in the cellular events of cell growth, survival, migration, and differentiation, through the sequential assembly of protein interactions, which form signal transduction pathways. However, the role of proteins in many cellular events remains unknown. Among a variety of methods to uncover protein function, chemical genetics is a remarkable approach in which small molecular compounds are used as probes to elucidate protein functions within signaling pathways.[2,3] Indeed, several bioactive compounds have led to breakthroughs in understanding the functional roles of proteins. For example, the study of chemical genetics using FK506, which was isolated from a microbial origin as a new immunosuppressant,[4] contributed to the identification of the important role of calcineurin in the immune system, by identifying FKBP12 as a target protein of FK506.[5,6] Another example is the discovery of lactacystin, a new microbial metabolite which induces differentiation in neuroblastoma cells,[7] whose target identification drove the wide application of lactacystin as a proteasomal inhibitor in the field of cell biology.[8–10] There are now a growing number of chemical inhibitors of signal transduction pathways, and these examples demonstrate how chemical genetics can lead us towards understanding cellular events at a molecular level. However, one significant hurdle to developing new chemical probes of biological systems is identifying the target protein of bioactive compounds, discovered using cell-based small-molecule screening. Identification of the molecular target of bioactive compounds is the major barrier to advancing chemical genetic research. This review therefore aims to describe approaches for identifying these molecular targets.

A variety of methods and technologies for identifying target proteins have been reported. These can be fundamentally categorized into two approaches: direct and indirect.[11] In the direct approach, proteins bound to each compound are purified and directly identified using time-of-flight mass spectrometry (TOF/MS) analysis. Compounds are immobilized using affinity beads or columns to purify the bound proteins (Fig. 1A and Table 1). In this respect, chemical synthesis of the compounds would become a great help for the preparation of the immobilized compounds. However, in the case of natural products, this synthesis is sometimes difficult because of the chiral centers and unique scaffolds in their structures.

On the other hand, the indirect approach offers target candidates by profiling the biological data of the compounds.[11] In the case that the compound was found to perturb some cellular event whose regulatory signaling pathways had been already reported, by clarifying which step within the pathway was affected by the compound, the enzymatic protein engaged in this step could be raised as the target candidate of the compound. In some cases, '-omics' studies (e.g., proteomics, transcriptomics) can help to collect comprehensive data about the biological effects of particular compounds to aid target profiling (Fig. 1B and Table 1).

2. Direct approach

Traditional approaches using affinity chromatography, biochemical fractionation, and radioactive ligand binding assays have been successful in identifying the biological targets of multiple

* Corresponding author.
E-mail address: imoto@bio.keio.ac.jp (M. Imoto).

0968-0896/$ - see front matter © 2011 Elsevier Ltd. All rights reserved.
doi:10.1016/j.bmc.2011.10.081

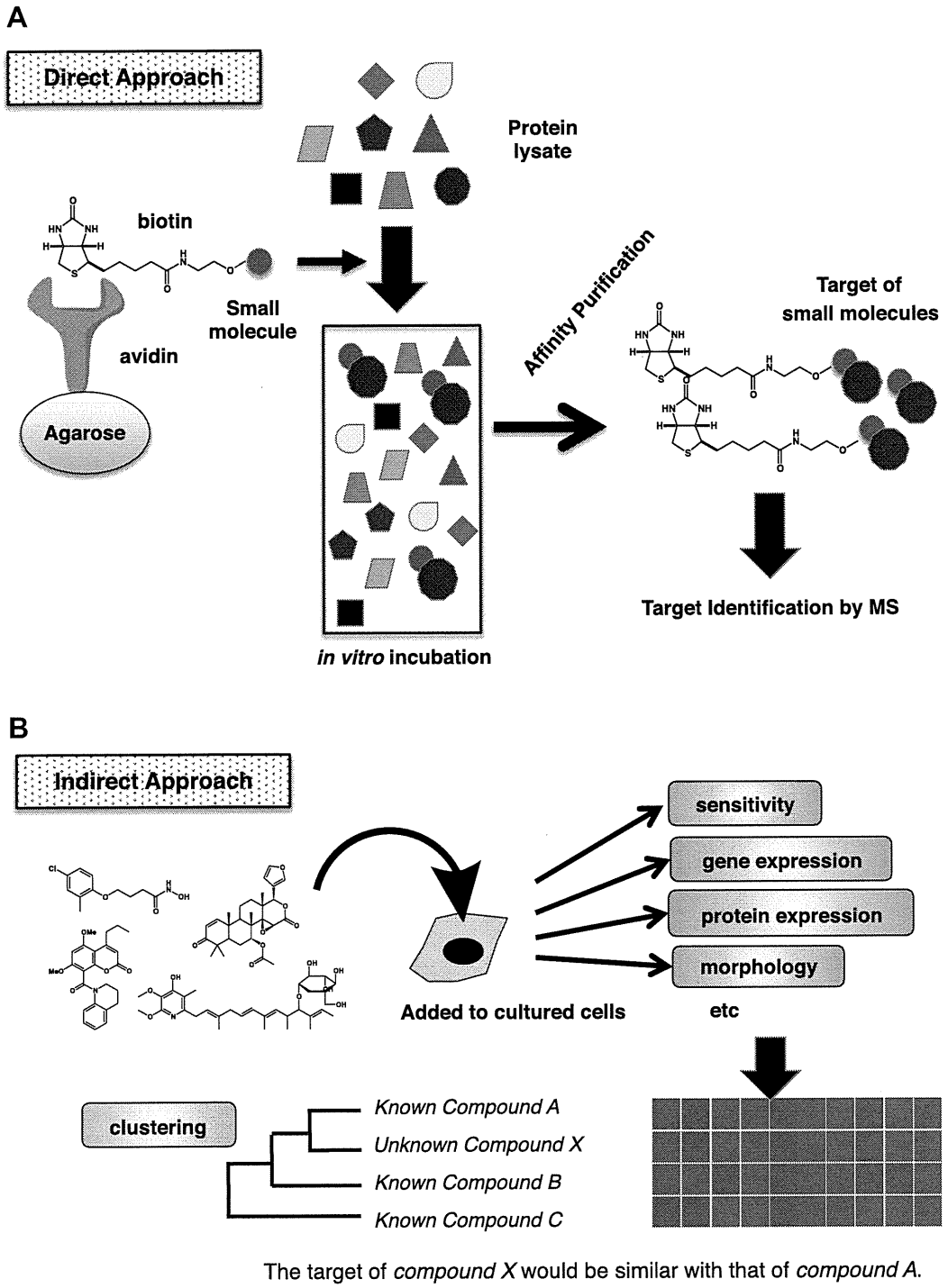

Figure 1. Schematic illustration of 'Direct Approach' and 'Indirect Approach'. (A) The strategy of target identification by using biotin-affinity tags is shown. Cell lysates are incubated with biotin-tagged small molecules and the binding-protein is purified with avidin-agarose before identification using mass spectrometry (MS). (B) The strategy of target identification by profiling is shown. Target-known and target-unknown small molecules are added to cultured cells and the cellular responses, such as drug sensitivity, gene expression, protein expression, or morphological changes, are collected. The profiling from the collected data predicts the target of the small molecule of interest.

small molecules. In particular, affinity chromatography using a biotin affinity tag or Affi-gel system has been successful, but is disadvantaged by the fact that small molecules can lose their biological activity due to the presence of the biotin affinity tag or Affi-gel tag at the active site. To overcome this issue, new methods such as click chemistry, photo-crosslink, and FG beads are now in development. This section highlights recent successes using affinity chromatography as the 'Direct approach'.

2.1. Biotin affinity tag

Target identification using a biotin-affinity tag was first developed by Professor Stuart L. Schreiber.[12] At present, this method was believed to be a powerful tool to identify target proteins. Indeed, many target proteins have since been identified using this method, including target proteins of chromeceptin,[13] withaferin A,[14] tetrahydroisoquinoline,[15] spliceostatin,[16] pladienolide,[17] and

fatostatin[18] (Fig. 2). Chromeceptin was identified as an inhibitor for insulin-induced adipogenesis,[19] and was suggested to exert its biological activity by blocking the autocrine loop of IGF2. Furthermore, chromeceptin activates the transcription factor STAT6, resulting in up-regulation of IGFBP-1 (IGF binding protein 1) and SOCS-3 (suppressor of cytokine signaling 3). IGFBP-1 is known to be a secreted IGF-binding polypeptide which inhibits IGF2. On the other hand, SOCS-3 is reported to suppress insulin-induced tyrosine phosphorylation of insulin receptor substrate (IRS-1), causing insulin resistance. Therefore, chromeceptin was suggested to inhibit insulin-induced adipogenesis through STAT6-stimulated IGFBP-1 and SOCS-3 up-regulation. However, its precise mechanism of action was unknown. Uesugi and co-workers identified MFP-2 (multifunctional protein 2), which is involved in the peroxisomal β-oxidation of fatty acids, as a chromeceptin-binding protein by affinity purification using biotinylated-chromeceptin.[13] Knockdown of MFP-2 suppressed chromeceptin-increased IGFBP-1 expression. These results collectively suggest that MFP-2 is essential for chromeceptin-induced STAT6 activation. Their study provided chemical genetic support for the role of the STAT-SOCS pathway in IGF regulation, and implicated a new pathway for STAT6 activation.

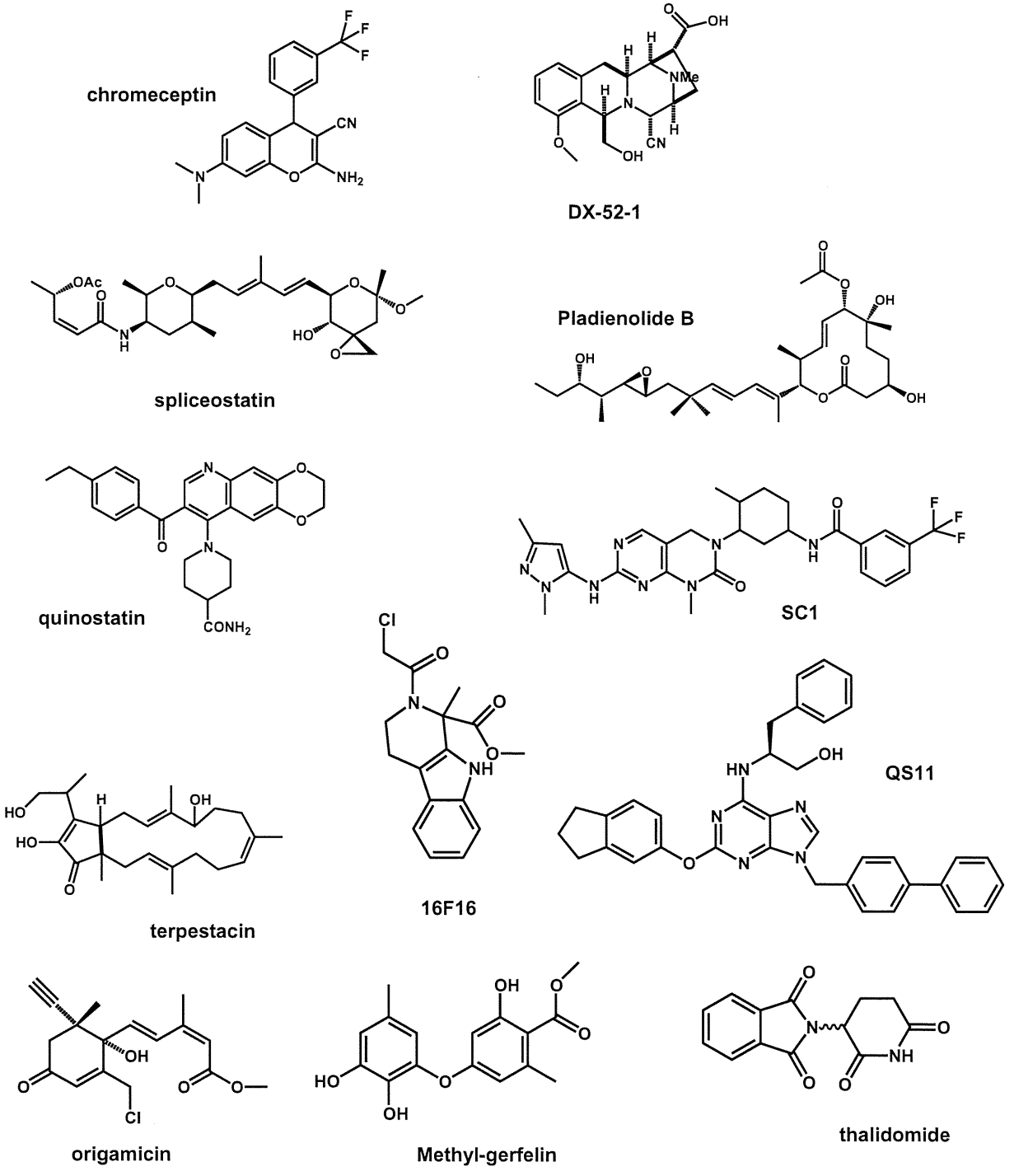

Figure 2. Structure of small molecules whose targets were identified by the 'Direct Approach'.

Table 1
Summary of small molecules whose targets were identified by the 'Direct Approach' or the 'Indirect Approach'

Method category		Compound name	Original bioactivity	Target protein	Journal	First author	Year
Direct approach	Biotin-affinity tag	Chromeceptin	Anti-adipogenesis	MFP-2	Chem. Biol.	Yongmun Choi	2006
		Withaferin A	Anti-cell migration	Annexin-II	Nat. Chem. Biol	Ryan R. Falsey	2006
		DX-52-1	Anti-cell migration	Radixin	Chem. Biol.	Alem W. Kahsai	2006
		DX-52-1	Anti-cell migration	Galectin-3	J. Biol. Chem.	Alem W. Kahsai	2008
		Spliceostatin	Anti-tumor	SF3b	Nat. Chem. Biol.	Daisuke Kaida	2007
		Pladienolide	Anti-tumor	SF3b	Nat. Chem. Biol.	Yoshihiko Kotake	2007
		Fatostatin	Anti-adipogenesis	SCAP	Chem. Biol.	Shinji Kamisuki	2009
	Affi-Gel tag	SC1	Regulation of self-differentiation of ES cells	RasGAP/ERK1	PNAS	Shinji Kamisuki	2009
		Quinostatin	mTOR inhibitor	PI3K p110	Chem. Biol.	Jiong Yang	2007
		QS11	TCF transcriptional activation	ARFGAP1	PNAS	Qisheng Zhang	2007
	Phage display	Terpestacin	Anti-angiogenic	UQCRB (mitochondrial complex III)	J. Biol. Chem.	Hye Jin Jung	2010
	Click chemistry	Origamicin	Anti-HCV activity	PDI	Chem. Biol.	Bojana Rakic	2006
		16F16	Anti-huntingtin	PDI	Nat. Chem. Biol.	Benjamin G. Hoffstrom	2010
	Photo-crosslink	Methyl-gerfelin	Anti-cell migration	Glyoxalase I	PNAS	Makoto Kawatani	2008
	FG-beads	Thalidomide	Teratogenicity	Cereblon	Science	Takumi Ito	2010
Indirect approach	DARTS	Resveratrol	Antioxidant	eIF4A	PNAS	Brett Lomenick	2009
	COMPARE analysis	ZSTK474	Kinase inhibitor	PI3K	J. Netl. Can. Inst.	Shin-ichi Yaguchi	2006
	Connectivity Map	Gedunin	Anti-malarial activity	HSP90	Cancer Cell	Haley Hieronymus	2006
		Celasteol	Growth inhibition	HSP90	Cancer Cell	Haley Hieronymus	2006
		Droxinostat	Enhancing CH-11-induced apoptosis	HDAC	Mol. Cancer Ther.	Tabitha E. Wood	2010
	Proteomic profiling	BNS-22	Growth inhibition	Topoisomerase II	Chem. Biol.	Makoto Kawatani	2011
	Morphological profiling	Pseudolarix acid B	Anti-fungal activity	Microtubule	Nat. Chem. Biol.	Daniel W. Young	2008
		Bisebromoamide	Cytotoxicity	Actin	ACS Chem. Biol.	Eriko Sumiya	2011
		Miuraenamide A	Anti-fungal activity	Actin	ACS Chem. Biol.	Eriko Sumiya	2011
	Metabolomic profiling	Glucopiericidin A	Filopodia inhibition	Glucotransporter	Chem. Biol.	Mitsuhiro Kitagawa	2010
	Chemical-genetic profiling	Papuamide B	Anti-HIV activity	Phosphatidylserine	Cell	Ainslie B. Parsons	2006
		Leucascandrolide	Cell growth inhibition	Cytcrome bc1 complex	Nat. Chem. Biol.	Olesya A. Ulanovskaya	2008
		Theonellamide F	Anti-fungal activity	3β-Hydroxysterols	Nat. Chem. Biol.	Shinichi Nishimura	2010

Tetrahydroisoquinoline DX-52-1, a semi-synthetic derivative of quinocarmycin, was identified as an inhibitor of cell migration.[20] By using biotinylated-DX-52-1, Fenteany and co-workers reported that radixin was the primary target of DX-52-1.[20] Radixin is a member of the ezrin/radixin/moesin (ERM) family of membrane-actin cytoskeleton linker proteins,[21] and ERM family proteins have been reported to bind to actin and various cell adhesion molecules, such as CD44. To elucidate the involvement of radixin in DX-52-1-inhibited cell migration, the authors investigated the effects of DX-52-1 on cell migration in radixin-overexpressing or radixin-knockdown cells. Overexpression of radixin made cells less sensitive to the anti-migratory activity of DX-52-1, whereas radixin knockdown using siRNA resulted in a reduced rate of cell migration, suggesting that radixin plays an important role in DX-52-1-inhibited cell migration. To further address the biological function of radixin in DX-52-1-inhibited cell migration, the authors examined the interaction between radixin and actin or CD44. They found that DX-52-1 disrupted radixin's ability to interact with both actin and CD44, which resulted in an inhibition of cell migration. On the other hand, although radixin was the most intensely labeled protein by biotinylated-DX-52-1, three other less intensely labeled proteins were also detected. Further research aimed at identifying these other proteins found that galectin-3, a family of lectins, was a secondary target of DX-52-1.[15] Similar to radixin, overexpression of galectin-3 decreased sensitivity to the anti-migratory activity of DX-52-1, whereas knockdown of galectin-3 resulted in decreased cell motility and cell adhesion. These results also suggested that galectin-3 plays an important role in DX-52-1-inhibited cell migration. However, the functional correlation between radixin and galectin-3 in cell motility and cell adhesion remains unclear.

The natural product FR901464 was isolated from a fermentation broth of the bacterium *Pseudomonas* sp. as an anti-cancer compound that enhances the transcriptional activity of the SV40 promoter, causes cell cycle arrest at the G1 and G2/M phases,[22,23] and induces abnormal mRNA splicing. However, the molecular mechanism of FR901464 was unknown. Yoshida et al. performed a SAR study to identify which moiety of FR901464 could be attached to biotin, without losing its biological activity. They succeeded in synthesizing a more potent methyl ketal derivative of FR901464, named spliceostatin, and also in synthesizing biotinylated-spliceostatin. By using biotinylated-spliceostatin, they were able to identify the SF3b complex, a subcomplex of the U2 small nuclear ribonucleoprotein (snRNP) in the spliceosome, as a target of spliceostatin. As SF3b has an important role in the U2 snRNP, which binds to the mRNA branchpoint sequence, spliceostatin